NRIAG Journal of Astronomy and Geophysics 6 (2017) 434–451

Contents lists available at ScienceDirect

NRIAG Journal of Astronomy and Geophysics

journal homepage: www.elsevier.com/locate/nrjag

Full length article

Modeling of geoelectric parameters for assessing groundwater potentiality in a multifaceted geologic terrain, Ipinsa Southwest, Nigeria – A GIS-based GODT approach

Kehinde Anthony Mogaji *, Osayande Bright Omobude

Department of Applied Geophysics, Federal University of Technology, P.M.B. 704, Akure, Nigeria

ARTICLE INFO

Article history:
Received 25 April 2017
Revised 12 June 2017
Accepted 11 July 2017
Available online 12 August 2017

Keywords:
Groundwater potential index
GIS
Geophysics
GOD model
Hard rock terrain
Analytic hierarchy process
GODT

ABSTRACT

Modeling of groundwater potentiality zones is a vital scheme for effective management of groundwater resources. This study developed a new multi-criteria decision making algorithm for groundwater potentiality modeling through modifying the standard GOD model. The developed model christened as GODT model was applied to assess groundwater potential in a multi-faceted crystalline geologic terrain, southwestern, Nigeria using the derived four unify groundwater potential conditioning factors namely: **G**roundwater hydraulic confinement (G), aquifer **O**verlying strata resistivity (O), **D**epth to water table (D) and **T**hickness of aquifer (T) from the interpreted geophysical data acquired in the area. With the developed model algorithm, the GIS-based produced G, O, D and T maps were synthesized to estimate groundwater potential index (GWPI) values for the area. The estimated GWPI values were processed in GIS environment to produce groundwater potential prediction index (GPPI) map which demarcate the area into four potential zones. The produced GODT model-based GPPI map was validated through application of both correlation technique and spatial attribute comparative scheme (SACS). The performance of the GODT model was compared with that of the standard analytic hierarchy process (AHP) model. The correlation technique results established 89% regression coefficients for the GODT modeling algorithm compared with 84% for the AHP model. On the other hand, the SACS validation results for the GODT and AHP models are 72.5% and 65%, respectively. The overall results indicate that both models have good capability for predicting groundwater potential zones with the GIS-based GODT model as a good alternative. The GPPI maps produced in this study can form part of decision making model for environmental planning and groundwater management in the area.

1. Introduction

The effect of climate change among other factors on the hidden earthly mineral resources cannot be overemphasized (Bates et al., 2008; Mogaji et al., 2013). Such effect had caused severe stress on the often available surface water particularly in a crystalline basement complex geologic terrain causing its paucity resulting from its dried up during dry season and degrading of surface water quality status via air pollution etc (Anomohanran et al., 2017). But then, for the reasons of all kinds of domestic, agricultural and industrial water demands, the inadequacies of surface water resource are largely met by groundwater supplies (Machiwal and Singh, 2015; Srivastava et al., 2012). In the studies of Fitts (2002), Todd (2004) and Oseji and Ofomola (2010), groundwater is described as water in the saturated zone which fills the pore spaces among mineral grains or cracks and fractured rocks within rock mass. The formation of groundwater derives its origin from rain or snow melts which seeps down through the soil into the underlying rocks (Saraf and Choudhury, 1998 and Banks et al., 2002). Its occurrences and accumulation is always at deeper depth in the earth subsurface and thus cannot be seen directly with

* Corresponding author.
E-mail addresses: mogakeh@yahoo.com (K.A. Mogaji), omobudebright222@gmail.com (O.B. Omobude).

Peer review under responsibility of National Research Institute of Astronomy and Geophysics.

Production and hosting by Elsevier

http://dx.doi.org/10.1016/j.nrjag.2017.07.001
2090-9977/

naked eye (Jha et al., 2010). This perhaps often complicated the quantification of its accumulation potentiality in an area of interest.

Generally, in a crystalline complex geologic terrain, groundwater productivity potential are restrained within fractured and weathered formation (Machiwal and Jha, 2014). Geologically, such fractured and weathered formation are referred to as aquifer formation (Faleye and Olorunfemi, 2015 and Kayode et al., 2016). In accordance with Satpathy and Kanungo (1976), Dan-Hassan and Olorunfemi (1999), and Bala and Ike (2001), such possible aquifer formations which can either be unconfined or confined types in a complex geologic terrain are often localized and discontinuous. The varying physical properties of these aforementioned aquifer types including porosity, permeability, transmissivity etc largely determined the groundwater potentiality of an area (Olorunfemi and Fasuyi, 1993 and Faleye and Olorunfemi, 2015). Such haphazard aquifer hydraulic properties variation that characterized the crystalline Basement rock complex terrain could have been responsible for the low success rate of most drilled holes (Mogaji, 2016a). As such, several scientific approaches have been investigated to salvage the spate borehole failures in similar complex geologic areas. This is with the view to develop reliable decision support model tool viable for optimizing groundwater productivity exploration at when due. The prominent of such approaches include hydro-geological, geophysical prospecting, remote sensing/GIS technique and multi-criteria decision analysis techniques (Jha et al., 2010, 2007; Meijerink, 2007; Kayode et al., 2016; Mogaji, 2016b and Mogaji and Lim, 2017b).

The application of multi-criteria decision analysis (MCDA) techniques in the field of groundwater hydrology is relatively a recent development. However, the uniqueness of these MCDA techniques' philosophy is such that their mechanisms allow systemic analysis and integrating of relevant criteria/factors to model or predicting target proposition that are traceable to mineralization potential mapping, groundwater potentiality mapping, vulnerability mapping etc (Elmahdy and Mohamed, 2014; Corsini et al., 2009; Carranza et al., 2008; Mogaji, 2017). Among the mostly used MCDA methods in groundwater prospectivity mapping is the analytical hierarchic processes (AHP) approach (Adiat et al., 2012; Chowdhury et al., 2009; Jha et al., 2010; Mogaji and Lim, 2016). According to these studies, many factors believed to be influencing or controlling groundwater potential i.e. groundwater potentiality conditioning factors (GPCFs) often served as input indices synthesized for groundwater potentiality zones prediction in the investigated areas (Adiat et al., 2012; Jha et al., 2010). To mention few of the commonly used GPCFs input indices are lithology, drainage pattern, lineament density, soil and topographic slope, geoelectrical parameters (lithology layer's resistivity and thickness) etc (Akinlalu et al., 2017; Mogaji and Lim, 2016; Adiat et al., 2013). The combination of those used GPCFs for the potential zones modeling was effectively carried out through exploring the potential of the MCDA - AHP systemic approach. With this approach, the considered GPCFs' spatially dependent subjectivity relative to their degrees of relevance to potential mapping within a short distance were harmonized and this has contributed to developing reliable potential zones prediction's decision model in those studies. Referencing the unique role of the applied MCDA technique, a more reliable DSS model map for precise decision making in environmental studies compared to the traditional means of inferring decisions based on single factor/parameter commonly obtained from interpreted geophysical, hydrogeological/borehole and satellite data has been established (Adiat et al., 2013; Pathak et al., 2015). The GOD model among other overlay and index-based methods invented by Foster (1987) is another MCDA systemic technique whose proficiency has been reported in groundwater vulnerability modeling (Andreo et al., 2005). Besides, for the purpose of precise decision making in groundwater recharge zones prediction, the applicability of the GOD modeling algorithm has been explored (Cheng-Haw et al., 2013). Thus, the efficiency of GOD model in groundwater sustainability management through its mapping potential of groundwater recharge and vulnerability zones which according to Mogaji et al. (2015b) and Mogaji (2017) are the very keys to groundwater resources development has been feasible. GOD model derived its acronyms from three basic criteria including: the groundwater hydraulic conferment (G), the overlying lithology strata (O) and the depth to water table (D) that have direct bearing with groundwater conduit movement and accumulation in the subsurface (Jha et al., 2010 and Adeyemo et al., 2015). These aforementioned GOD model's criteria are attainable from many data sources such as geophysical, hydrogeological/borehole and satellite measurement survey project (Gorai et al., 2014; Mogaji and Lim, 2016). For instance, in the study of Khemiri et al. (2013), the adopted GOD model approach derive its criteria from hydrogeological/borehole data sources. However, as reported in the studies of Jha et al. (2010) and Adiat et al. (2012), the hydrogeological/borehole data sources is very costly, time–consuming, non-invasive and most importantly, it lack regional prospectivity mapping. Thus, a concept of reviewing and exploring the potentiality indexing mapping of the conventional GOD model algorithm through deriving these modeling criteria, i.e. the G, O, D elements from geophysical approach point of view and the additional introduction of aquifer thickness (T) criterion, which is one of the major driven parameter that controls the occurrence, movement and accumulation of groundwater in an area (Oh et al., 2011; Mogaji and Lim, 2016) are considered in this study.

The potentials of geophysical method has been highly relevant in subsurface investigations (Vladimir et al., 2017). This may not be unconnected to its non-invasive/non-destructive, less risky and cost-effective unique attributes (Mogaji et al., 2015b; Olayanju et al., 2017). The measurable physical properties of the earth superficial materials obtainable based on a practical applied geophysical method have served as input for GPCFs modeling in some number of studies (Adiat et al., 2013; Mogaji, 2016a,b; Jha et al., 2010). Further, the application of geophysical techniques have gained widespread acceptance in groundwater resource exploration (Mohamed et al., 2012). Few of these geophysical prospecting methods include electromagnetic, magnetic, seismic refraction, electrical resistivity etc (Sultan and Santos, 2009; Sharma and Barawal, 2005; Gruba and Rieger, 2003; Jupp and Vozoff, 1975). Among these aforementioned prospective geophysics methods, the direct-current electrical resistivity (ER) method is the most highly efficient in groundwater studies. The ER method uniqueness in the field of hydrogeophysics is such that it has ability to map both geological layers as well as determining the nature and composition of unseen subsurface formations (Fitterman et al., 2012; Hinnell et al., 2010). Besides, there exist a close relationship between the ER method's interpreted geoelectrical parameters and the physical electrical conductivity properties of the subsurface formations. Some of the proficiency of ER method practical applications in groundwater resource exploration include mapping and delineation of prolific aquifer formation, quantitative estimate of the water-transmitting properties of the mapped aquifer units etc (Oborie and Udom, 2014; Mogaji, 2016a). Besides, these possible ER method's geoelectrical parameters including aquifer thickness, aquifer resistivity, anisotropy coefficient, longitudinal conductance etc formed the origin of the derived GPCFs as used in the studies of Jha et al. (2010), Adiat et al. (2013), Mogaji (2016b) for groundwater potential zones prediction modeling. However, it is important to note that the produced groundwater potentiality index model in these priors studies were based on multi-criterially synthesizing and modeling of the geoelectrical derived-GPCFs through potential application of GIS technique.

Sequel to this, the advent of geospatial technologies including the remote sensing and geographical information system (GIS) techniques have indeed been explored and their contributions in the field of groundwater hydrology are enormous (Mogaji and Lim, 2017a; Nampak et al., 2014; Awawdeh et al., 2014; Machiwal and Singh, 2015; Singh et al., 2014). Deducing from those previous works, the effective application of the above discussed MCDA models in environmental decision making process are carried out in GIS platform. This perhaps is because the geographic information system (GIS) technique can effectively handle large amounts of spatial data, which are traceable to potentiality and vulnerability modeling analyses. This unique attribute of GIS approach has largely enhanced the efficient implementation of various MCDA models (Manap et al., 2011; Adiat et al., 2012; Park et al., 2014; Mogaji and Lim, 2016). Thus, the potential of GIS technique as a vital tool for driven the proposed multi-critically-based GODT model will be acknowledged in this study.

The present study attempt developing a MCDA-based GODT model for regional assessment of groundwater potentiality in a Precambrian basement complex geologic terrain via exploring the integration of geophysical and GIS techniques. The geoelectrical derived GPCFs input for the proposed GODT modeling algorithm are G (Groundwater hydraulic conferment), O (Overlying lithology strata), D (Depth to water table and T (aquifer Thickness). The specific objectives of this study are as follows: (i) generate hydrologic maps for the derived GPCFs inputs in GIS environment, (ii) determined the groundwater potentiality prediction index (GPPI) estimates from multi-criterially synthesizing of the G, O, D, and T maps through applying the GODT modeling algorithm, (iii) process the GPPI estimates to produce groundwater potentiality prediction zones map in GIS environment, (iv) Validate the produced GPPI maps using the available well data and geologic information obtainable in the area. (v) Carry out comparative study between the proposed GODT model and the applied results of the standard simple weighted AHP-MCDA model with the view of establishing the proficiency of the proposed model in groundwater resources management and sustainability through validating the output decision making model maps.

2. The study area description

The study area is situated near Akure metropolis covering the northeastern part of Ipinsa community in the southwestern part of Nigeria. From the cardinal measurement, the area lies between latitude 735,200 and 736,800 and longitude 809,200 and 810,400 (Fig. 1a). The topographical terrain analysis of the area established its undulating nature to be of surface elevation ranging between 379 m and 429 m. The available climatic information for the area established that the wet season often begins mid-April and ends October with an average rainfall of about 1524mm, while the dry season do starts around November and ends in March with an average atmospheric temperature between 28 °C and 31 °C and a mean annual relative humidity of about 80 percent (en.wikipedia.org/wiki/Akure). Geologically, the study area is underlain by

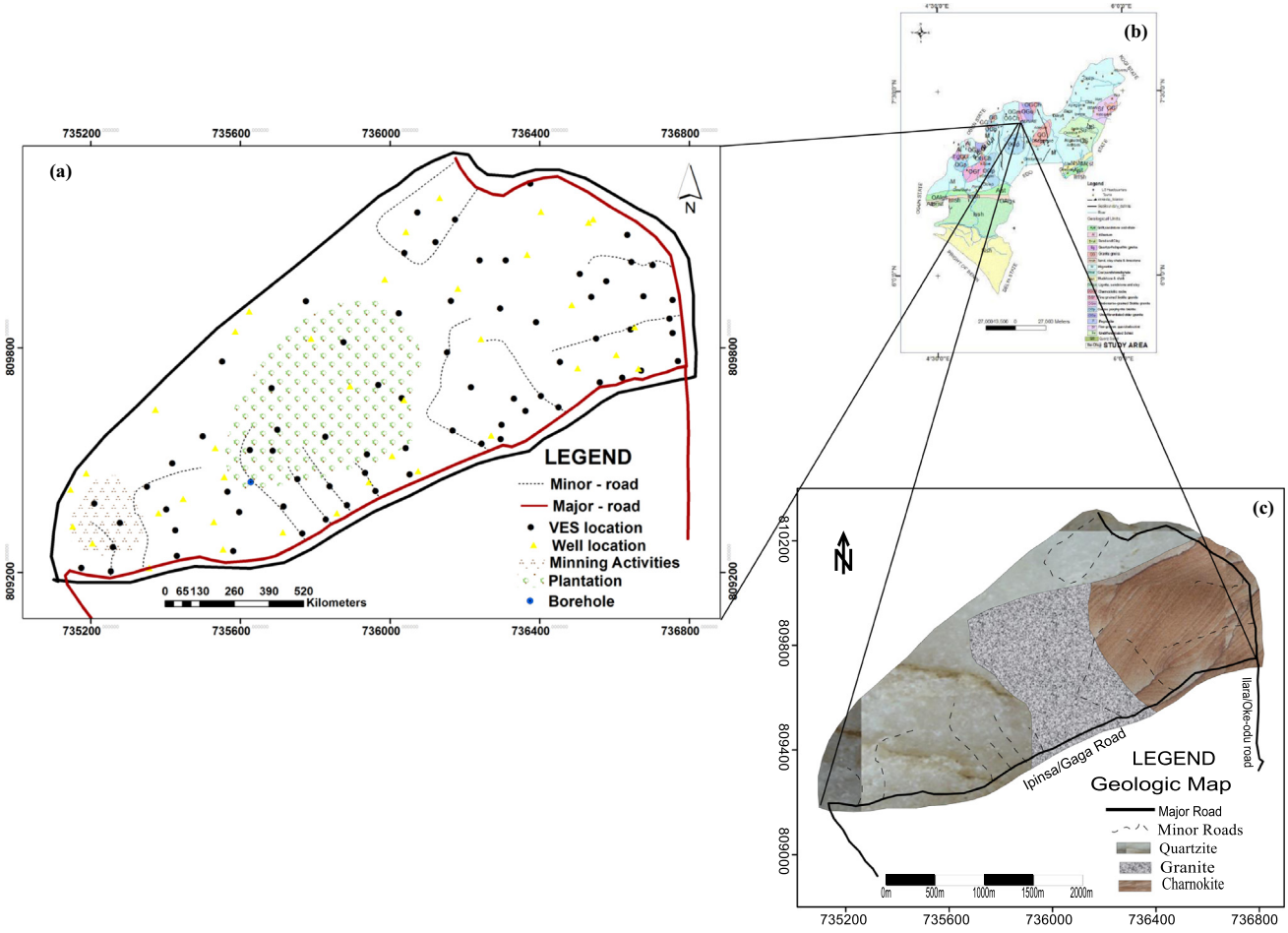

Fig. 1. The location maps showing (a) Site map of the study area displaying the data acquisition locations and other relevant features; (b) geological map of Ondo State and (c) site local geological map.

the Precambrian Basement Complex rocks of Southwestern, Nigeria as depicted in Fig. 1b. The three lithologic units recognized in the area include; the quarzitic, the granitic and the charnockites rock types shown in Fig. 1c. The co-existence of these varying geologic rock units largely contribute to the complexity difficulty usually encounter during mapping and delineation of prolific aquifer units that are often localized and discontinuous (Satpathy and Kanungo, 1976). The mirroring of the geologic properties of the subsurface materials that overlie and constitute the underlain aquifer units through applying the state-of-the art approach can largely provide in situ information for accurate location of prolific aquifer zones with little or no biasness in any investigated area.

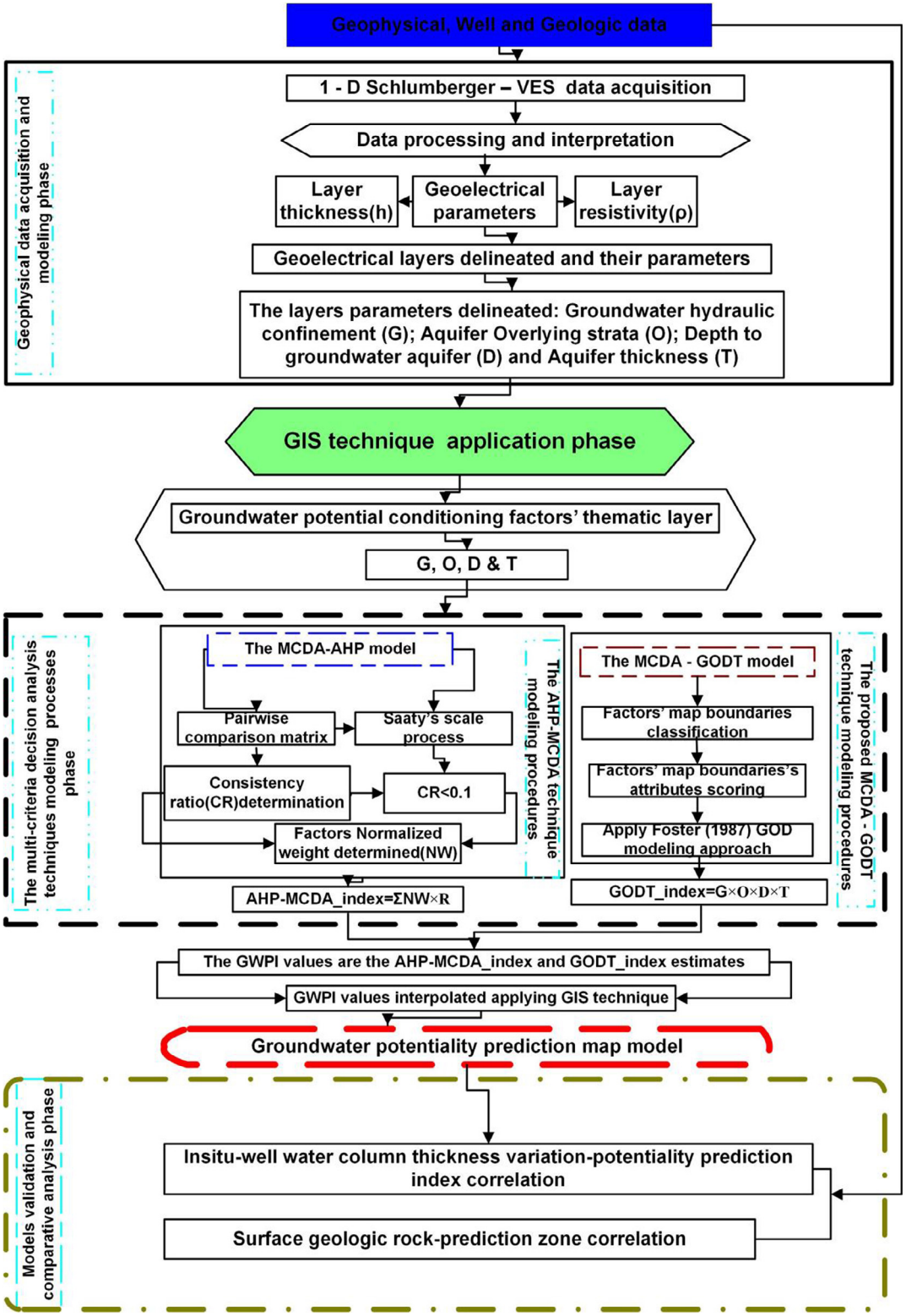

Fig. 2. The adopted methodology flowchart for the study.

3. Materials and methodology

The materials used in this study encompass the obtained well data measurement records, the geologic data and the field acquired geophysical data. In order to achieve the set objectives of this work, the flow of the adopted methodology is presented in Fig. 2. The methodological steps followed are grouped into five. In step 1, the field geophysical data acquisition and geoelectrical parameter modeling were carried out. Step 2, the potential of GIS technique modeling application was explored. This was followed by implementing the theory and principle of the proposed GODT model as well as investigating the AHP–MCDA technique in groundwater potentiality assessment. The production of groundwater potential prediction index (GPPI) map through the applied GODT model algorithm proposed make up the 4th steps. The last step involved the validation of the GODT model-based GPPI map and comparatively analysis of its prediction capability with that of the applied MCDA-AHP model in the same task are evaluated. The details of each segments are as highlighted in the following subsection.

3.1. The geophysical data acquisition and modeling phase

3.1.1. Geophysical data acquisition

The electrical resistivity method involving the deployed of Vertical Electrical Sounding (VES) technique using the Schlumberger electrode configuration was adopted for data acquisition at 73 locations in the study area (Fig. 1a). At each occupied locations, the R-50 DC Resistivity meter was used to measure the apparent resistivity values. The spread length of the Schlumberger current electrode varies between 2 m and 300 m. The Global Positioning System (GPS) device was used to record the geographical coordinates (in degrees) of the occupied VES stations.

3.1.2. Data processing, interpretation and geoelectrical layer parameters delineation

The acquired Schlumberger VES data were processed by plotting the measured apparent resistivity values against the half current electrode spacing (AB/2) at each station on a log-log graph sheets to generate the resistivity field curves. The produced field curves were curve-matched using manual interpretation being done with the help of standard master curves (Orellana and Mooney, 1966; Rijkswatersta, 1969). These interpreted results were further refined and iterated with the help of WinResist™ version 1.0 of Vander-Velper (2004). For the purpose of ensuring reasonable analysis and interpretation of the acquired geophysical survey data, the preview into the available drilled bore well litho logs information from the neighborhood surroundings were used as a control and constraint for defining the lithologic layer's boundary beneath each occupied VES locations. Presented in Fig. 3, are the typical plotted VES data field curves displaying the geoelectrical parameters (apparent resistivity values and thicknesses) which quantitatively defined the delineated subsurface lithologic layers occasioned at various depths in the area. The summary of the interpreted geoelectrical parameters and the inferred interpreted subsurface lithologic layers are presented in Table 1. Furthermore, in order to derive the relevant groundwater potential conditioning factors (GPCFs) as inputs for implementing the proposed GODT model's algorithm, the determined geoelectrical parameters assisted with the interpreted subsurface lithologic description (Table 1) were further remodeled to define (i) Groundwater

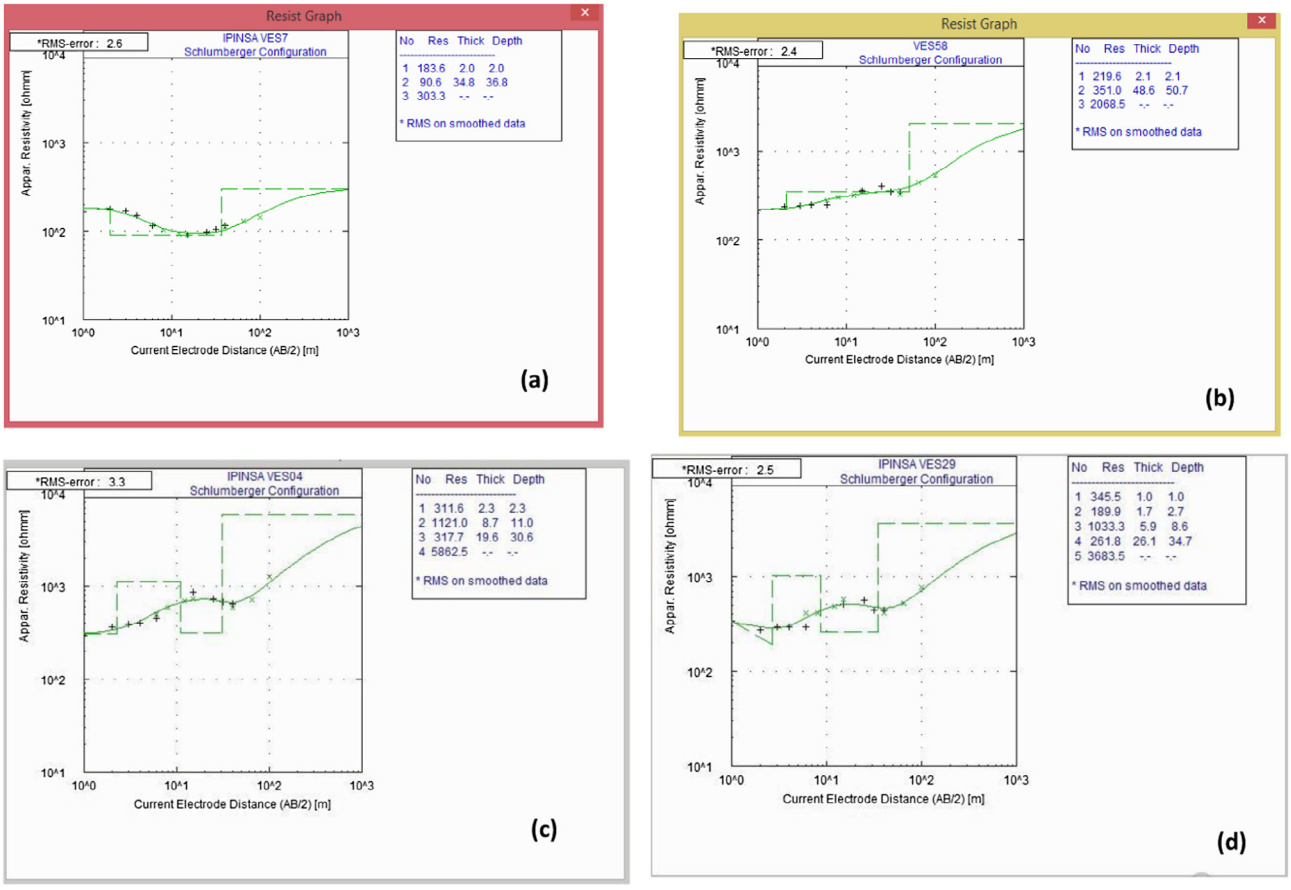

Fig. 3. Typical resistivity model curves obtained in the area; (a) H type, (b) A type, (c) KH type and (d) HKH type.

Table 1
The determined geoelectrical parameters and their defined lithologic layers.

VES no	Type curves	Resistivity ($\rho_1 \ldots \rho_n$)Ωm//thickness ($h_1 \ldots h_n$)m	Interpreted subsurface lithological description
1	H	56,23,256//1.2,1.9	Clayey topsoil, sandy clay
2	KH	91,2460,269,1532//1.2,2.4,38.3	Clayey topsoil, laterite, sandy clay
3	KH	128,2728,366,15075//1.1,1.1,23.3	Clay sandy, topsoil, laterite, sandy clay
4	KH	312,1121,318,5883//2.3,8.7,19.6	Sandy clay topsoil, laterite, sandy clay
5	KH	138,470,169,1337//2.9,12.3,41.5	Clayey topsoil, fractured laterite, sandy clay
6	KH	168,700,44,18396//4.6,0.7,24.1	Clay sandy topsoil, fractured laterite, clay
7	H	184,91,303//2.0,34.8	Clay sandy topsoil, clay, Fractured bedrock
8	A	76,632,9999//1.1,11.1	Clay topsoil, fractured unit
9	KH	103,390,83,1250//1.5,3.4,11.6	Clay topsoil, weathered laterite, clay, fractured bedrock
10	KH	47,990,137,1498//3.0,3.5,39.3	Clay topsoil, fractured laterite, weathered clay
11	KH	139,696,39,1634//0.6,2.9,13.2	Clay sandy topsoil, fractured laterite, clay
12	H	394,49,1726//6.7,18.2	Sandy clay topsoil, clay
13	KH	215,2127,19,1339//1.2,2.3,17.6	Sandy clay topsoil, laterite, Clay
14	KH	224,796,77,1396//2.7,9.1,27.0	Sandy clay topsoil, laterite, sandy clay
15	KH	473,3130,108,2111//0.4,8.8,18.4	Sandy clay topsoil, laterite, clay sandy
16	KH	313,934,50,2192//2.5,11.6,16.2	Sandy clay topsoil, fracture laterite, clay
17	KH	215,1400,346,1844//1.1,4.5,59.2	Sandy clay topsoil, laterite, sandy clay
18	KH	160,350,70,544//2.0,1.5,6.5	Sandy Clay topsoil, fractured laterite, clay, fractured bedrock
19	KH	210,431,246,1345//1.1,2.0,14.8	Sandy clay topsoil, fractured laterite, sandy clay
20	KH	190,974,388,14616//0.6,2.3,7.3	Sandy clay topsoil, fractured laterite, sandy clay
21	KH	172,3082,276,787//1.7,6.9,10.5	Sandy clay topsoil, laterite, sandy clay
22	H	94,67,3487//1.3,3.6	Clay topsoil, clay
23	A	104,497,3033//2.2,6.9	Sandy clay topsoil, fractured unit
24	H	80,20,2783//0.7,1.2	Clay topsoil, clay
25	H	157,126,2752//1.1,3.2	Sandy clay topsoil, sandy clay
26	H	161, 70, 2033//1.1,1.2	Sandy clay topsoil, clay
27	KH	129,659,240,4601//1.0,0.9,3.7	Clay sandy topsoil, fracture laterite, sandy clay
28	A	46,114,3429//1.3,3.1	Clay topsoil, clay sandy
29	HKH	346,190,1033,262,3684//1.0,1.7,5.9,26.1	Sandy clay topsoil, weathered material, laterite, sandy clay
30	KH	63,282,191, 8726//1.2,1.0,29.0	Clay topsoil, weathered laterite, sandy clay
31	KH	34,1615,235, 4606//0.4, 2.5,9.4	Clay topsoil, laterite, sandy clay
32	KH	167,1464,122,2528//1.4,10.1,19.7	Sandy clay topsoil, laterite, clay sandy
33	KH	244,1940,62,3764//3.9,8.0,12.6	Sandy Clay topsoil, laterite, Clay
34	A	149,216,46792//0.5,5.2	Clay sandy topsoil, sandy clay
35	A	44,189,20274//0.4,4.6	Clay topsoil, sandy clay
36	KH	77,805,68,66342//0.4,0.5,1.1	Clay topsoil, fractured laterite, clay
37	HKH	248,77,3574,156,5953//0.5,1.0,1.9,2.0	Sandy clay topsoil, weathered clay, laterite, clayey sand
38	A	58,208,43205//1.8,0.9	Clay topsoil, sandy clay
39	A	90,1893,12487//1.3,0.3	Clay topsoil, boulder
40	H	209,51,21530//0.5,0.6	Sandy clay topsoil, weathered clay
41	KH	46,303,93,378//0.6,6.2,36.1	Clay topsoil, weathered laterite, clay
?	?	?	?
?	?	?	?
72	A	48,271,15066//1.3,4.3	Clay topsoil, sandy clay
73	QH	2107,1114,52,2056//2.1,14.6,22.9	Hard topsoil, laterite, clay

hydraulic confinement i.e. the aquifer types (G), (ii) aquifer unit Overlying strata (O), (iii) Depth to groundwater aquifer unit top (D) and (iv) aquifer unit Thickness (T) characterizing the study area. Table 2 presents the result of the derived GPCFs. The modeling criteria for the area aquifer types classification is as presented in Table 3. Column 2 of this table has the ranges of resistivity parameter values revealing the nature of superficial materials that overlies the area aquifer units mapped. Using the resistivity ranges, the area areas underlain aquifers were classified into four groups. For the superficial materials having ≥100 Ωm or <600 Ωm, are less resistive and higher recharge ability compare to that with <100 Ωm or ≥1000 Ωm. However, a moderate resistive and low recharge covered materials is attributed to unit with ≥600 Ωm or <1000 Ωm and this defined the semi-confined aquifer types. The above adopted modeling criterion is relatively in agreement with findings of Olorunfemi and Fasuyi (1993).

3.2. Application of GIS tool

The philosophy of the mostly used multi-criteria decision analysis (MCDA) models is such that their background algorithms has functionality to synthesize maps of varying parameters relevant to target proposition. In this study, the maps/layers for the derived geoelectrical-based GPCFs/parameters as aforementioned were produced through spatial modeling of the records in Table 2 using the kriging interpolation technique of the geostatistical wizard module in GIS environment. Fig. 4, presents the GPCFs' thematic maps produced. The maps were the inputs modeling criteria considered for implementing proposed GODT and AHP modeling algorithms. It should be noted that the selected GPCFs was informed by the GOD model's algorithm requirement. But then, the aquifer unit thickness (T) thematic parameter was considered for the GOD model's algorithm enhancement. Thus we have the modified GODT model's algorithm. The hydrological significance of these selected GPCFs have been discussed in the studies of Mogaji et al. (2011), Adiat et al. (2013), Jha et al. (2010), Mogaji (2016a,b). According to Fig. 4, the spatial attributes of these factors in respect of their relevant towards groundwater occurrences assessment are varied from one place and largely space dependent (Jha et al., 2010; Machiwal et al., 2010; Manap et al., 2011; Adiat et al., 2012; Mogaji and Lim, 2016). The concept of harmonizing these factors' varying degree of hydrological influence in producing a reliable decision support system (DSS) model for mapping groundwater potential zones in the investigated area is the laudable task in this study. To achieve this task, the functionality of the proposed GODT modeling algorithm and its comparative application results with

Table 2
The summary of the derived GPCFs for the adopted MCDA modeling algorithms.

VES no	Easting	Northing	Elevation	G	O	D	T
1	735253.5	809202.3	392	NN	56.00	1.20	1.90
2	735,259	809,267	399	C	1276.00	3.60	38.30
3	735,278	809,332	408	C	1428.00	2.20	23.30
4	735,209	809,384	409	C	717.00	11.00	19.60
5	735,350	809,429	406	U	304.00	12.30	29.30
6	735,426	809,312	394	SC	434.00	5.20	24.10
7	735,581	809256.5	401	U	184.00	2.00	34.80
8	735,597	809,361	401	C	76.00	1.10	10.00
9	735,765	809303.4	390	U	247.00	4.80	11.60
10	735,752	809,449	398	SC	519.00	6.50	39.30
11	735,686	809,525	400	SC	418.00	3.50	13.20
12	735,551	809,763	398	U	394.00	6.70	18.20
13	735,775	809,925	401	C	1171.00	3.60	14.10
14	735,683	809,692	407	SC	510.00	9.10	27.00
15	735,876	809,815	418	C	1802.00	9.20	18.40
16	736,023	809,892	414	SC	624.00	14.10	16.20
17	736,038	810,054	415	C	808.00	5.60	59.20
18	736,042	809,532	409	U	255.00	3.60	6.90
19	735,418	809,491	399	U	647.00	3.10	14.80
20	735,938	809,515	410	SC	582.00	2.20	18.60
21	735,827	809,562	416	C	1627.00	2.60	10.50
22	736,362	809,631	407	C	94.00	1.30	3.60
23	736,331	809,664	409	U	104.00	2.20	6.90
24	736,403	809,671	403	NN	80.00	0.70	1.20
25	736,454	809,762	415	U	158.00	1.10	3.20
26	736,747	809,878	408	NN	161.00	1.10	1.20
27	736,769	809764.4	409	SC	394.00	1.90	3.70
28	736560.7	809707.5	404	NN	46.00	1.30	3.10
29	736,298	809,594	414	C	523.00	8.60	26.10
30	736244.9	809543.3	409	U	173.00	2.20	29.00
31	736,174	810,143	405	C	825.00	2.90	9.40
32	736,121	810,083	410	C	817.00	11.60	19.70
33	736,073	810,162	403	C	1092.00	11.80	12.60
34	736,309	810,034	417	U	149.00	0.50	5.20
35	736,634	810,102	405	C	44.00	0.40	4.60
36	736,239	810,034	417	NN	441.00	0.90	0.50
37	736,152	809,788	412	C	1300.00	3.40	2.00
38	736,645	810,030	425	NN	58.00	1.80	0.90
39	736,538	809,936	417	NN	86.00	1.30	0.80
40	736,507	809,998	415	NN	209.00	0.50	0.60
41	735,499	809,563	396	U	175.00	6.80	36.10
?	?	?	?	?	?	?	?
?	?	?	?	?	?	?	?
72	736,755	809,840	425	C	48.00	1.30	4.30
73	735,625	809,527	406	C	1611.00	16.70	22.90

G: groundwater reservoir conferment; **O**: Aquifer Overlying strata resistivity; **D**: Depth to groundwater aquifer top; **T**: Aquifer unit thickness; **U:** Unconfined aquifer; **SC**: Semi-unconfined aquifer; **C**: Confined aquifer and **NN**: Non-aquifer; GPCFs: Groundwater potential conditioning factors.

Table 3
The modelling criteria for the area mapped aquifer types (modified after Olorunfemi and Fasuyi, 1993).

S/N	Aquifer overlying resistivity (Ωm)	Groundwater Hydraulic Confinement	Symbol
1	≥100 or <600	Unconfined	U
2	≥600 or <1000	Semi-unconfined	SU
3	<100 or ≥1000	Confined	C
4	0	Non-aquifer	NN

U: Unconfined aquifer; **SC**: Semi-unconfined aquifer; **C**: Confined aquifer and **NN**: Non-aquifer.

the applied results of the existing simple weighted AHP-MCDA modeling algorithm were analyzed and processed in GIS environment.

3.3. The theories and principles of the applied MCDA Models

3.3.1. The GODT modeling approach

GODT model is an index overlay data mining approach. The theoretical mechanism of this model takes its origin from the GOD model (Foster, 1987). According to Foster (1987), this is a rating system method that can process and standardize scoring values derived from its required input parameters. In this study, the required parameters for the proposed GODT model are as discussed above. In order to produce decision making index model using these GPCFs, the GODT model algorithm was applied to harmonize multi-criterially their relative importance towards groundwater potentiality mapping and an estimated model's aggregate index results climax the processes. Involving the GIS application in the GODT modeling application greatly easy its regional prospectivity mapping. Thus for the established GODT-based estimated aggregate index results mostly obtained from the combined GPCFs' maps, a regional prospectivity model map can be prepared through applying the geostatistical wizard module in GIS environment. Mathematically, the standard synthesizing mechanism algorithm relationship for the proposed GODT model modified after Andreo et al. (2005) and Adeyemo et al. (2015) is expressed in Eq. (1)

$$\text{GODT\_index} = G \times O \times D \times T \quad (1)$$

where **G:** groundwater hydraulic confinement; **O:** aquifer overlying strata; **D:** depth to groundwater aquifer top; **T:** aquifer unit thickness.

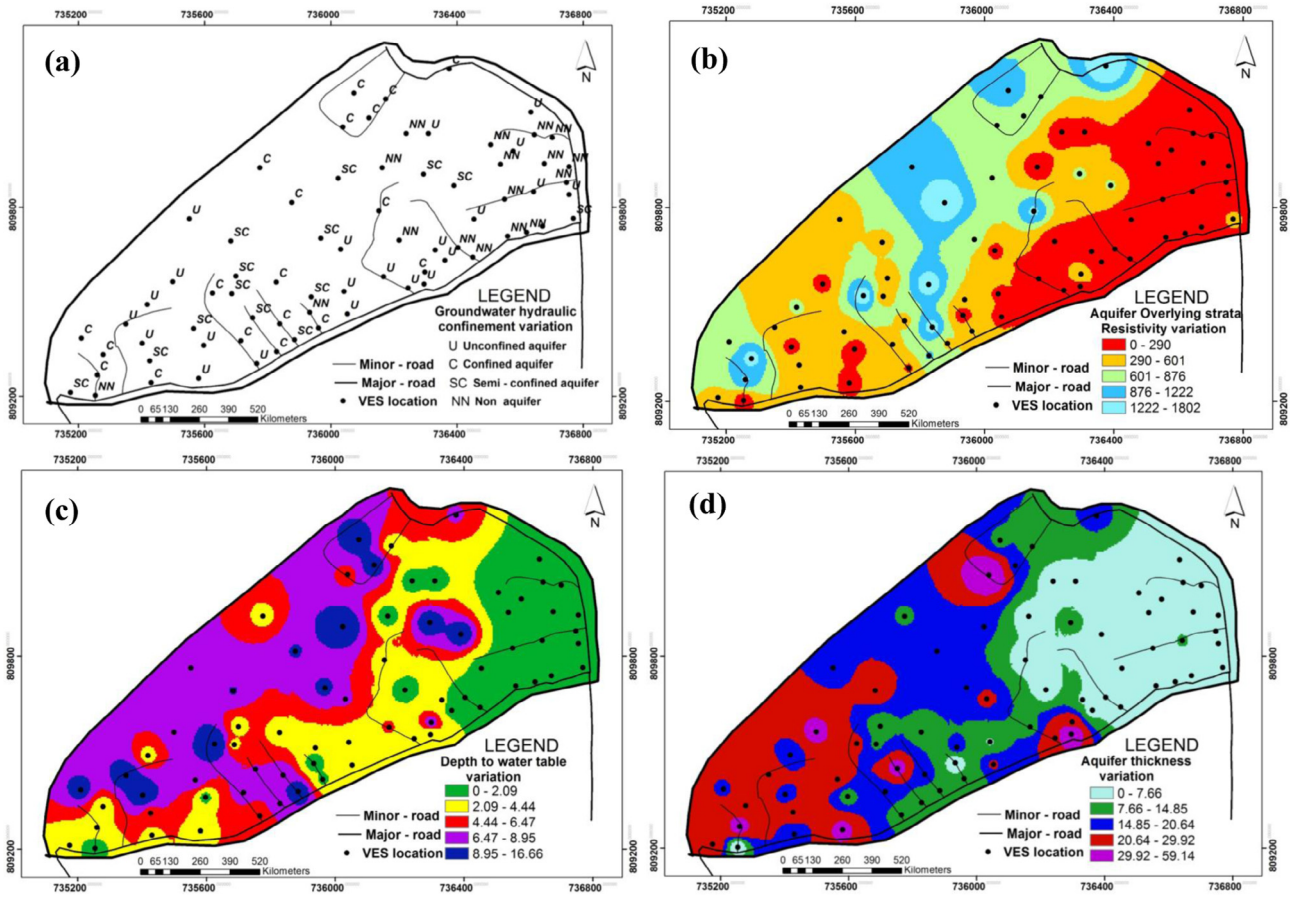

Fig. 4. The GPCFs thematic parameter layers produced for the applied GODT and AHP MCDA models (a) groundwater hydraulic conferment (**G**); (b) Aquifer Overlying strata resistivity (**O**); (c) Depth to groundwater aquifer top (**D**); (d) Aquifer unit thickness (**T**).

Table 4
A matrix of pair-wise comparisons of groundwater potential conditioning factors (GPCFs) for the AHP process.

Pairwise comparison 9 point continuous rating scale								
Less important				More important				
1/9 Extremely	1/7 Very strongly	1/5 Strongly	1/3 Moderately T	1 Equally G	3 Moderately O	5 Strongly D	7 Very strongly Weights	9 Extremely CR
T			1	3	3	5	0.42	0.074
G			1/3	1	3	5	0.35	
O			1/3	1/3	1	3	0.15	
D			1/5	1/5	1/3	1	0.08	
Column total			1.8667	4.533	7.333	14	1	

G: groundwater hydraulic confinement; **O:** aquifer overlying strata; **D:** depth to groundwater aquifer top; **T:** aquifer unit thickness.

Table 5
The adapted Scoring attribution Notes fathomed for the GODT Model–based GPCFs' parameter maps (modified after Khemiri et al. (2013)).

G	Note	O (Ω-m)	Note	D (m)	Note	T (m)	Note
NN	0	34–339	0.4	0.4–2.82	1	0.53–8.34	0.07
C	0.2	339–637	0.5	2.82–5.31	0.9	8.34–15.24	0.13
SC	0.3–0.5	637–901	0.7	5.31–7.48	0.8	15.24–20.99	0.2
U	0.6–1	901–1233	0.8	7.48–9.90	0.7	20.99–30.18	0.27
		1233–1802	0.6	9.90–16.66	0.6	30.18–59.14	0.33

G: Groundwater hydraulic confinement; **O**: Aquifer overlying strata formation; **D**: Depth to aquifer and **T**: aquifer unit thickness; NN: Non-Aquifer; C: Confined Aquifer; U: Unconfined Aquifer and SC: Semi-confined Aquifer.

3.3.2. The AHP-MCDA technique

This is a knowledge driven multi-criteria mining technique that is potentially bias in human input or requiring of expert input in its efficacy application for environmental decision making (McKay and Harris, 2015). The operation mechanism of AHP-MCDA method is largely driven by Saaty scale standard. As reported in the study of Akinlalu et al. (2017), the Saaty has suggested the scale standard to be of 5 point calibration (1-3-5-7-9). Using this scale

Table 6
The score/rate scaling records based on the applied GODT modeling mechanism.

VES no	Eastings	Northings	G	O	D	T
1	735,254	809,202	0.00	0.40	0.60	0.07
2	735,259	809,267	0.20	0.80	0.70	0.33
3	735,278	809,332	0.20	0.80	0.60	0.27
4	735,209	809,384	0.20	0.50	1.00	0.20
5	735,350	809,429	0.60	0.40	1.00	0.27
6	735,426	809,312	0.30	0.50	0.70	0.27
7	735,581	809,257	0.60	0.40	0.60	0.33
8	735,597	809,361	0.60	0.40	0.60	0.13
9	735,765	809,303	0.60	0.40	0.70	0.13
10	735,752	809,449	0.30	0.50	0.80	0.33
11	735,686	809,525	0.30	0.50	0.70	0.13
12	735,551	809,763	0.60	0.50	0.80	0.20
13	735,775	809,925	0.20	0.80	0.70	0.13
14	735,683	809,692	0.30	0.50	0.90	0.27
15	735,876	809,815	0.20	0.60	0.90	0.20
16	736,023	809,892	0.30	0.50	1.00	0.20
17	736,038	810,054	0.20	0.70	0.80	0.33
18	736,042	809,532	0.60	0.40	0.70	0.07
19	735,418	809,491	0.60	0.50	0.60	0.13
20	735,938	809,515	0.30	0.50	0.60	0.20
21	735,827	809,562	0.20	0.60	0.60	0.13
22	736,362	809,631	0.60	0.40	0.60	0.07
23	736,331	809,664	0.60	0.40	0.60	0.07
24	736,403	809,671	0.00	0.40	0.60	0.07
25	736,454	809,762	0.60	0.40	0.60	0.07
26	736,747	809,878	0.00	0.40	0.60	0.07
27	736,769	809,764	0.30	0.50	0.60	0.07
28	736,561	809,708	0.00	0.40	0.60	0.07
29	736,298	809,594	0.20	0.50	0.90	0.27
30	736,245	809,543	0.60	0.40	0.60	0.27
31	736,174	810,143	0.20	0.70	0.60	0.13
32	736,121	810,083	0.20	0.70	1.00	0.20
33	736,073	810,162	0.20	0.80	1.00	0.13
34	736,309	810,034	0.60	0.40	0.60	0.07
35	736,634	810,102	0.60	0.40	0.60	0.07
36	736,239	810,034	0.00	0.50	0.60	0.07
37	736,152	809,788	0.20	0.80	0.80	0.07
38	736,645	810,030	0.00	0.40	0.60	0.07
39	736,538	809,936	0.00	0.40	0.60	0.07
40	736,507	809,998	0.00	0.40	0.60	0.07
41	735,499	809,563	0.60	0.40	0.80	0.33
42	735,699	809,581	0.30	0.40	0.70	0.07
43	735,885	809,379	0.30	0.50	1.00	0.13
44	735,838	809,430	0.20	0.60	0.90	0.20
45	735,933	809,466	0.00	0.40	0.60	0.20
46	735,961	809,417	0.20	0.50	0.60	0.07
47	736,167	809,579	0.60	0.40	0.70	0.13
48	736,031	809,666	0.60	0.40	0.80	0.27
49	735,968	809,701	0.30	0.50	1.00	0.20
50	736,450	809,641	0.00	0.40	0.60	0.07
51	735,175	809,212	0.30	0.50	0.60	0.27
52	735,402	809,368	0.60	0.40	1.00	0.20
53	735,430	809,243	0.00	0.50	0.70	0.20
54	735,715	809,376	0.00	0.50	0.90	0.20
55	735,828	809,341	0.00	0.70	0.90	0.07
56	735,565	809,415	0.30	0.50	0.90	0.27
57	736,052	809,461	0.60	0.40	0.70	0.27
58	736,295	809,556	0.60	0.40	0.60	0.33
59	736,671	809,739	0.00	0.40	0.60	0.07
60	736,294	809,905	0.30	0.50	1.00	0.13
61	736,163	809,925	0.00	0.70	1.00	0.13
62	736,375	810,239	0.20	0.60	0.80	0.20
63	736,551	809,825	0.00	0.40	0.60	0.07
64	736,755	809,928	0.00	0.40	0.60	0.07
65	736,217	809,695	0.00	0.40	0.60	0.07
66	736,621	809,720	0.00	0.40	0.60	0.07
67	736,643	809,849	0.60	0.40	0.60	0.13
68	736,677	809,938	0.00	0.40	0.60	0.07
69	736,702	810,021	0.00	0.40	0.60	0.13
70	736,578	809,978	0.60	0.40	0.60	0.07
71	736,390	809,869	0.30	0.50	1.00	0.07
72	736,755	809,840	0.60	0.40	0.60	0.07
73	735,625	809,527	0.20	0.60	1.00	0.27

G: groundwater reservoir conferment; **O**: Aquifer Overlying strata resistivity; **D:** Depth to groundwater aquifer top and **T:** Aquifer unit thickness.

Table 7
Probability weighted and rating (R) for the classes of the GPCFs produced hydrologic themes.

GPCFs hydrologic themes	Category (Classes)	Potentiality for groundwater storage	Rating (R)	Normalized weight (W)
Groundwater hydraulic confinement (G)	Unconfined aquifer	Very high	5	0.35
	Confined aquifer	High	4	
	Semi confined aquifer	Medium	3	
	Non aquifer	Low	2	
Aquifer overlying strata (O)	34–339	High	4	0.15
	339–637	Very high	5	
	637–901	Medium	3	
	901–1233	Low	2	
	1233–1802	Very low	1	
Water table depth (D)	0.4–2.82	Very high	5	0.08
	2.82–5.31	High	4	
	5.31–7.48	Medium	3	
	7.48–9.90	Low	2	
	9.90–16.66	Very low	1	
Aquifer thickness (T)	0.53–8.34	Very low	1	0.42
	8.34–15.24	Low	2	
	15.24–20.99	Medium	3	
	20.99–30.18	High	4	
	30.18–59.14	Very high	5	

GPCFs: groundwater potential conditioning factors.

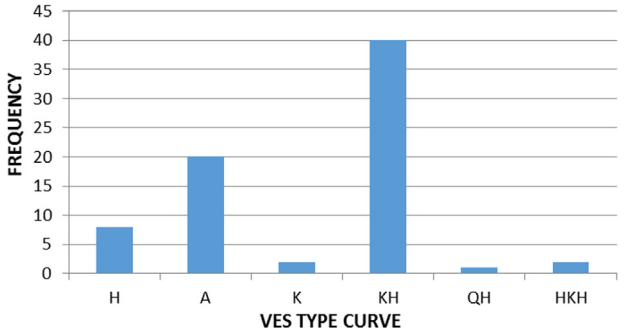

Fig. 5. Frequency chart for different VES-type curves obtained in the study area.

standard according to Saaty and Vargas (1991a,b), Pair-Wise comparison Matrices involving comparison of one criteria to one another can be constructed. Interpreting this scale was such that value of 1 suggests that one criterion is equally important to the paired criterion and a value of 9 leads one to infer that the criterion under consideration is extremely important in relation to the other criterion considered (Table 4). The pair-wise comparison technique represents a theoretically founded basis to compute weights indicating the relative importance of the criteria. The uniqueness of this model's theory application in environmental decision making process is that of its capability to computing the level of consistency in the pairwise comparison matrices via applying the model's sound mathematical basic equations as detailed in the studies of Zhou and Chen (2014), Mogaji and Lim (2016) and Akinlalu et al. (2017). The prepared Pair-Wise comparison Matrices for the selected GPCFs is shown in Table 4.

3.4. The applicability of GODT and AHP-MCDA models in groundwater potential mapping

The produced four geoelectrical parameters derived maps namely: the groundwater hydraulic confinement, aquifer overlying strata, depth to groundwater aquifer top and aquifer unit thickness (Fig. 4) referred to as GPCFs prepared for the area were used as input parameters for establishing the aptness of the GODT algorithm in groundwater potentiality assessment. With these GPCFs' themes also, the proficiency of the renowned AHP-MCDA technique was investigated. Firstly, the proposed GODT modeling mechanism was applied on each GPCFs' map representing the groundwater occurrence evidences, noting their varying degree of influence on the area groundwater storage potentiality. The spatial attributes of these GPCFs' map's boundaries considered in the GODT modeling mechanism was quantitatively evaluated through applying the attribution scoring scale presented in Table 5. Through using the attribution scale, the NOTE's values in columns 2, 4, 6 and 8 that defined the ranges of groundwater storage potentiality were assigned to each map's class boundaries in function of their influence on groundwater storage potential. With the application of these NOTE's interpretation scale, records of score/rate at each VES locations depicted on the GPCFs' thematic maps regarding the observed spatial attributes at each VES locations were obtained (Table 6). The established GODT modeling algorithm (Eq. (1)) was applied to synthesize the records (Table 6) in GIS environment to determine the GODT-based estimated aggregate index results. According to Adiat et al. (2012) and Mogaji (2016a,b), the GODT-based estimated aggregate index is synonymous to groundwater potential index (GWPI) quantitatively computed for the area. Thus, it was referred to as GODT model-based GWPI (Table 8). Secondly, the modeling algorithm of the AHP-MCDA method was equally used to evaluate these produced GPCFs maps. The applied AHP-MCDA model on these GPCFs was purposely used to estimate the groundwater potential index (GWPI) characteristics in the area. In order to integrate the effect of each GPCFs for determining the AHP- based GWPI values variation in the area, the established steps reported in the studies of Chowdhury et al. (2009), Jha et al. (2010), Mogaji and Lim (2016) were adopted. Table 7 gives the analysis of the effects of the selected GPCFs on groundwater storage potentiality. The established AHP-MCDA index modeling algorithm for estimating GWPI in the field of groundwater hydrology is given in Eq. (2):

$$GWPI = G_W G_R + O_W O_R + D_W D_R + T_W T_R \quad (2)$$

where subscripts W and R are the normalized weights and ratings for each unify GPCFs, respectively. R in Eq. (2) define the ranges of groundwater storage potentiality within each unify GPCFs. The information for the applied AHP-MCDA index modeling algorithm (Eq. (2)) in groundwater potential mapping are provided in Table 7. According to this Table, the GPCFs' hydrologic themes' names and their classes/ranges are given in columns 1 and 2. Whereas, the Rat-

Table 8
The computed results of the GODT and AHP-MCDA modeling algorithms.

VES nos	Location's coordinates		GODT model-based	AHP model-based
	Long	Lat	GWPI values	GWPI values
1	735,254	809,202	0.00	1.80
2	735,259	809,267	0.04	3.46
3	735,278	809,332	0.03	2.96
4	735,209	809,384	0.02	3.16
5	735,350	809,429	0.07	4.43
6	735,426	809,312	0.03	4.07
7	735,581	809,257	0.05	4.53
8	735,597	809,361	0.02	3.27
9	735,765	809,303	0.02	3.77
10	735,752	809,449	0.04	4.49
11	735,686	809,525	0.01	3.15
12	735,551	809,763	0.05	4.00
13	735,775	809,925	0.02	2.20
14	735,683	809,692	0.04	4.15
15	735,876	809,815	0.02	2.78
16	736,023	809,892	0.03	3.51
17	736,038	810,054	0.04	3.76
18	736,042	809,532	0.01	2.93
19	735,418	809,491	0.02	3.20
20	735,938	809,515	0.02	3.49
21	735,827	809,562	0.01	2.12
22	736,362	809,631	0.01	2.85
23	736,331	809,664	0.01	2.85
24	736,403	809,671	0.00	1.80
25	736,454	809,762	0.01	2.85
26	736,747	809,878	0.00	1.80
27	736,769	809,764	0.01	2.65
27	736,561	809,708	0.00	1.80
28	736,298	809,594	0.02	3.80
29	736,245	809,543	0.04	4.11
30	736,174	810,143	0.01	2.50
31	736,121	810,083	0.03	3.16
32	736,073	810,162	0.02	2.59
33	736,309	810,034	0.01	2.85
34	736,634	810,102	0.01	2.85
35	736,239	810,034	0.00	1.95
36	736,152	809,788	0.01	1.78
37	736,645	810,030	0.00	1.80
38	736,538	809,936	0.00	1.80
39	736,507	809,998	0.00	1.80
40	735,499	809,563	0.06	4.69
41	735,699	809,581	0.01	2.73
42	735,885	809,379	0.02	3.39
43	735,838	809,430	0.02	2.78
44	735,933	809,466	0.00	3.06
45	735,961	809,417	0.00	3.00
46	736,167	809,579	0.02	3.77
47	736,031	809,666	0.05	4.27
48	735,968	809,701	0.03	3.51
49	736,450	809,641	0.00	1.80
50	735,175	809,212	0.02	4.33
51	735,402	809,368	0.05	4.01
52	735,430	809,243	0.00	3.22
53	735,715	809,376	0.00	3.38
54	735,828	809,341	0.00	2.24
55	735,565	809,415	0.04	4.15
56	736,052	809,461	0.05	4.19
57	736,295	809,556	0.05	4.53
58	736,671	809,739	0.00	1.80
59	736,294	809,905	0.02	3.39
60	736,163	809,925	0.00	2.39
61	736,375	810,239	0.02	2.70
62	736,551	809,825	0.00	1.80
63	736,755	809,928	0.00	1.80
64	736,217	809,695	0.00	1.80
65	736,621	809,720	0.00	1.80
66	736,643	809,849	0.02	3.27
67	736,677	809,938	0.00	1.80
68	736,702	810,021	0.00	2.22
69	736,578	809,978	0.01	2.85
70	736,390	809,869	0.01	2.97
71	736,755	809,840	0.01	2.85
72	735,625	809,527	0.03	3.28
73	735,254	809,202	0.00	1.80

Table 9
The characteristics of the groundwater potentiality maps based on the applied MCDA models.

Potential index classification	AHP model		GODT model	
	Range	Areal (%)	Range	Areal (%)
L	1.78–2.42	17	0.00–0.01	29
LM	2.42–2.97	30	0.01–0.02	24
M	2.97–3.55	29	0.02–0.03	31
H	3.55–4.69	24	0.03–0.07	16

L: Low; LM: Low-medium; M: Medium; H: High; MCDA: Multi-criteria decision analysis and AHP: Analytical Hierarchical Process.

ing (R) for the themes which defined the ranges of the potentiality for groundwater storage interpretation based on the order of each factors map's class boundary influences is given in column 4. In accordance with Al-Saud (2010) and Murthy (2000), the assigned rating scale R of 1 to 5 are interpreted as very low, low, medium, medium high, and high groundwater storage potentiality, respectively. The weights "W" in column 5 are the normalized weights for each GPCFs' themes determined based on the AHP approach discussed in Section 3.3.2. The "W" thus indicate their relative importance in contributing towards groundwater potentiality assessment in the area. In order to apply the GWPI algorithm given in Eq. (2) for GWPI index values computation, each VES locations depicted on the GPCFs' thematic maps (Fig. 4) were considered. The attributes of the observed location point reference to the class boundaries of any of the considered GPCFs' maps were interpreted vis-a-vis their corresponding groundwater potentiality interpretation as defined by the rating (R) scales assignment (Table 7). With the determined R and W variables at each criterion map observed location points, the linear additive combination of these variables using Eq. (2), the index (GWPI) values can be estimated.

4. Results and Discussion

4.1. The 1–D Schlumberger Depth sounding survey results

The Schlumberger Depth sounding results analysis carried out in this study were based on the inverted electrical sounding curves interpreted in form of the earth models. The generated geoelectric section earth models (not shown) often give insight into the subsurface structure and stratigraphy on the basis of the distribution of the interpreted geoelectrical resistivity values. The typical curve types obtained from the field measurements are shown in Fig. 3. The curve types range from simple 3-layer H type to complex 4-layers curves HKH type. According to Table 1, the records of the curve types characterizing the study area established that KH curve type is the most predominant among others (Fig. 5). This curve type being a combination of H and K curve types are typical curve types that revealed the complexity of crystalline multi-faceted geologic terrain (Jayeoba and Oladunjoye, 2013; Ndatuwong and Yadav, 2014; Kayode et al., 2016). Qualitatively, these curves types often gives mirror image of the successive lithologic sequence from

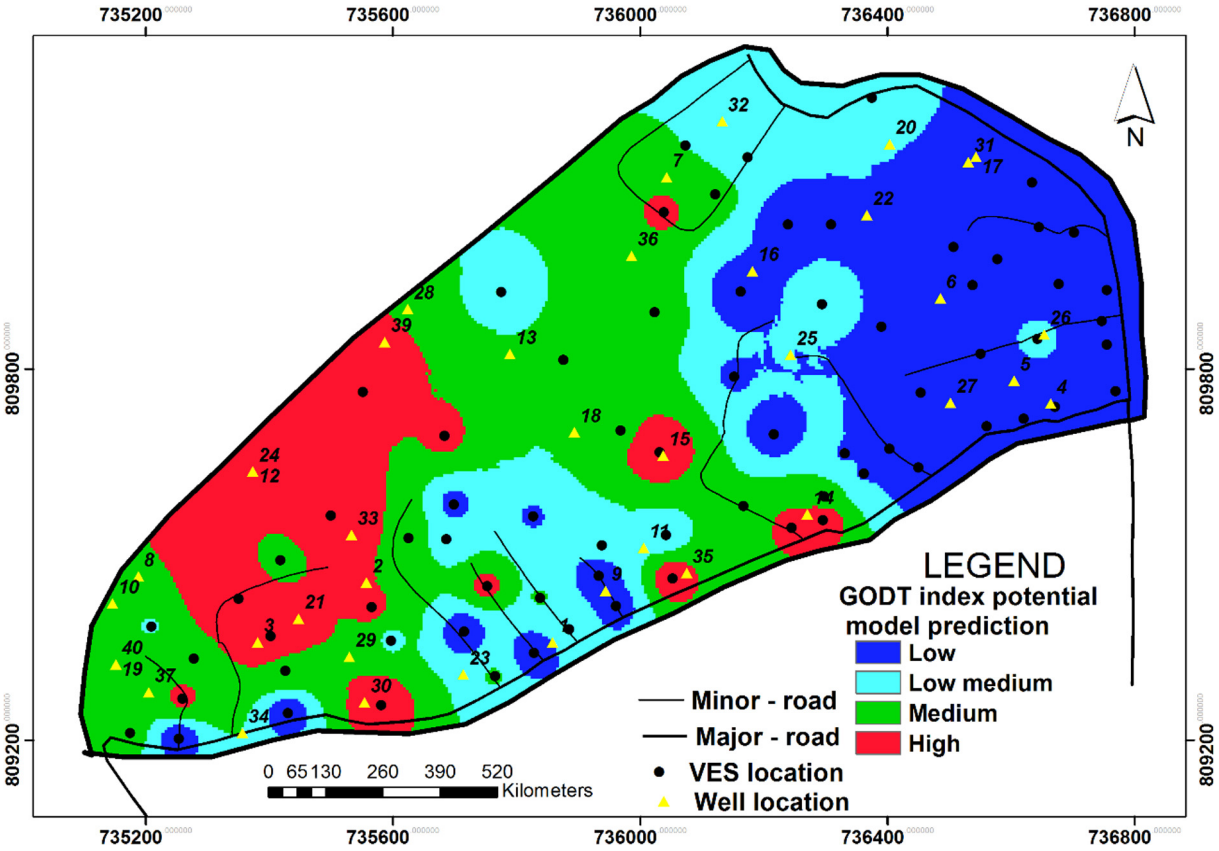

Fig. 6. Groundwater potential prediction index (GPPI) map based on GODT–MCDA model approach.

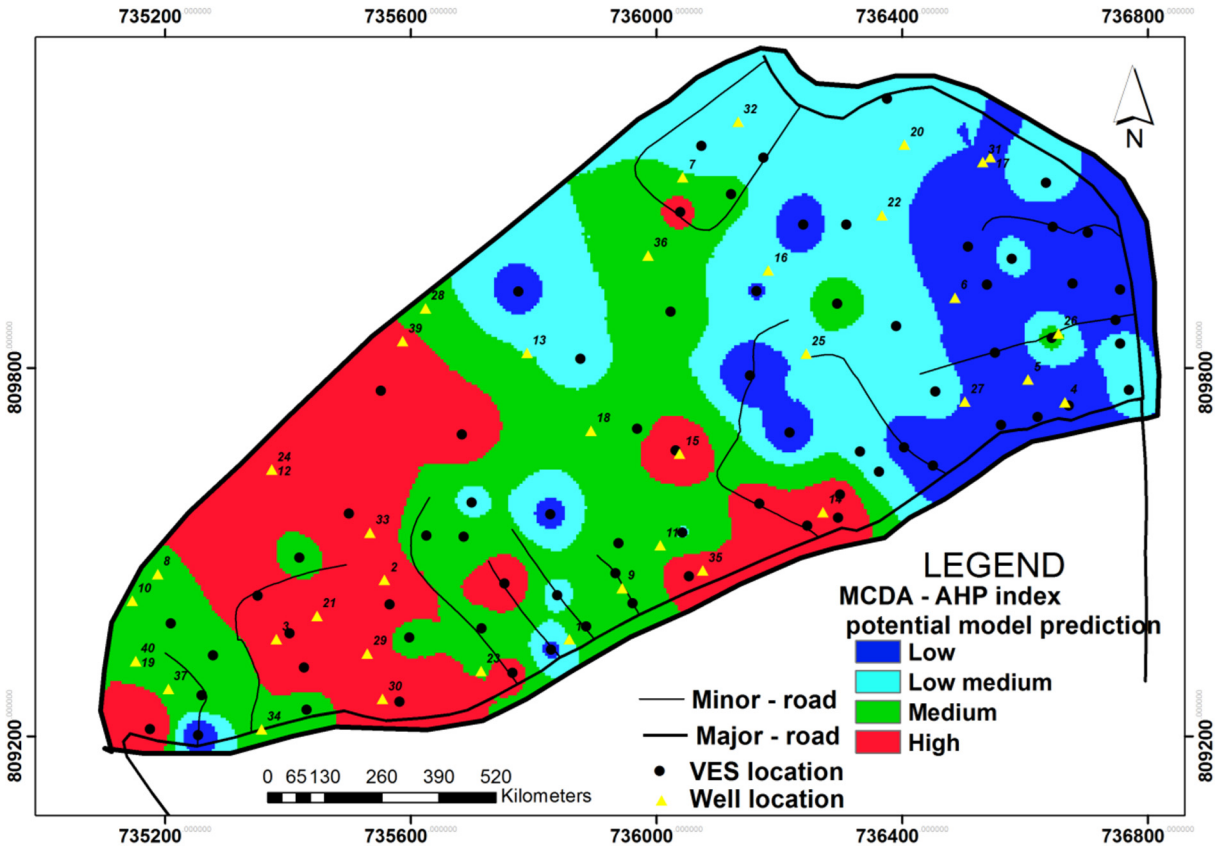

Fig. 7. Groundwater potential prediction index (GPPI) map based on AHP–MCDA model approach.

which physical properties of the material constituents of each identified lithological units can be interpreted for groundwater prospect of an area (Mogaji et al., 2011; Oladapo-Adeoye et al., 2015; Mogaji, 2016b). For the purpose of the precise subsurface lithological characterization, the information from the surrounding bore well litho-logs were used for constraining the VES data interpretation. The lithological sequence delineated in the area consist of topsoil, laterite, fractured/weathered materials and bedrock. The lithological sequence's interpreted geoelectrical parameters (resistivity, thickness) beneath each occupied VES location are in the range of (34–536 Ωm, 0.4–1.8 m), (659–12,601 Ωm, 0.5–11.4 m), (20–810 Ωm, 1.9–50.7 m) and (303–49,719 Ωm), respectively (Table 1). Table 1 records were further analyze to derive relevant hydrological factors for effective groundwater prospect assessment in the area. The results of the derived groundwater potential conditioning factors (GPCFs) based on the interpreted geoelectrical parameters are presented in Table 2. With the application of GIS tool, Table 2 results were spatially modeled to produce the GPCFs' thematic maps (Fig. 4a–d).

4.2. The GODT and AHP–MCDA models applications results in the groundwater potential prospecting

The application results of the proposed GODT and the surviving AHP–MCDA data mining models (Fig. 2) towards achieving these research objectives were reported in Tables 4, 5 and 7. According to Table 5, the records for the Note's columns, were the applied calibration scale for the GODT modeling mechanism. Each GPCFs' Note records indicate the groundwater potentiality interpreted results. For the **G** factor, the unconfined aquifer is assigned the highest potentiality result (0.6–1) compared to that of confined aquifer (0.2) (column 2). This is qualitatively due to the fact that the unconfined aquifer top is directly exposed to higher surface water recharge infiltration unlike the confined aquifer top (Sahoo et al., 2016a and Dhar et al., 2014). Further in the **O** factor's column, the numerical value 0.8 i.e. the Note column is assigned to the boundary class of 901–1233 Ω-m which is higher than 0.4 values assigned to the boundary class of 34–339 Ω-m. The reason is because the boundary class of 901–1233 Ω-m indicate relatively evidence of anomalous fractured features unlike the latter boundary unit that has clayey nature evidence in place. Regarding such 4th class boundary of O factor, the suspected fractured features can greatly enhance secondary porosity for higher groundwater potentiality unlike that of the clayey unit (the 1st class boundary) notable for low porosity and negligible permeability (Oladapo-Adeoye et al., 2015; Mogaji, 2016a,b). Further, in the case of depth to groundwater aquifer top (D) factor, considering the instance of deeper **D** estimate, the potentiality rate is often very low qualitatively, whereas high potentiality is attributed to a shallower D estimate as interpreted in column 6. For the aquifer units factors on the other end, the thicker boundary class unit (30.18–59.14 m) has the highest note value result while the thinner boundary unit (0.5–8.34 m) is assigned the lowest note value (Column 8). This is adduced to fact that a thicker aquifer unit is characterized with higher groundwater potentiality and vice-versa with thin aquifer unit bed (Jha et al., 2010; Adiat et al., 2013 and Mogaji and Lim, 2016). Implementing these interpreted records of GPCFs' Notes that have established the potentiality evaluation relevance of these influential factors through using of GODT model's principle and its algorithm Eq (1), the groundwater potential index beneath the VES locations were estimated. The determined GODT- based GWPI estimate beneath each occupied VES location are detailed in column 4 of Table 8. According to the Table, the GODT- based GWPI estimates for the area varies between 0.01 and 0.065. For the case of AHP–MCDA model on the other end, Tables 4 and 7 show the records of the application results. Column 5 of Table 7 gives the

determined normalized weight based on the AHP-MCDA modeling principle. Among the geoelectrical derived GPCFs, the aquifer unit thickness has the highest assigned weight (0.42) compared to the remaining factors' weights. Quantitatively, the aptness of T factor serving as the enhanced parameter in the proposed MCDA - GODT model is established. These determined GPCFs' weighting assignment established the varied degree of these unify factors' contributions towards groundwater potential occurrence in the area with the aquifer unit thickness having the highest influence. The appropriateness of the determined GPCFs' normalized weights (Column 5) is guided by the computed consistency ratio (0.074) shown in column 7 of Table 4. The multi-criterially analysis of the GPFCs for estimating groundwater potential index (GWPI) values characterizing the area was carried out employing the established Eq. (2). The AHP-MCDA based computed GWPI values records are presented in column 5 of Table 8. Table 8 established that the AHP-MCDA-based GWPI index values characterizing the study area are in the range of 1.78 to 4.68. This estimated AHP-MCDA- based GWPI is a relative measure of potentiality occurrence of groundwater in the area where areas with the higher index values have more potential rating, as compared with those with a lower index values (Chowdhury et al., 2009, Adiat et al., 2012; Mogaji and Lim, 2016).

4.3. The modeling of groundwater potentiality maps based on GODT and AHP-MCDA modeling application results

Table 8 shows the record of the estimated index values resulting from the applied MCDA models in the study area. From the table, Columns 4 and 5 were processed in GIS environment to spatially model the estimated index attributes of the area via adopting the quantile classification technique used in the studies of Rahmati et al. (2016) and Naghibi et al. (2015). Through using the classification ranges in column 2 and 4 of Table 9, the area groundwater potentiality prediction index (GPPI) maps were produced in GIS environment. The produced maps demarcate the area into four classes of potential zones namely; Low, Low-medium, Medium and High (column 1 of Table 9). Figs. 6 and 7 present GODT-MCDA model based map and AHP–MCDA model based map, respectively. The analyzed results of Figs. 6 and 7 for the corresponding areal coverage and percentage in each predicted groundwater potential zones category are detailed in Table 9. Based on this table, the GODT model-based GWPI produced map, the lows potential classes (L and LM) account for area coverage of about 53% while the predicted areas for both M and H potential classes cover 31% and 16%, respectively. Similarly, on the AHP-MCDA-

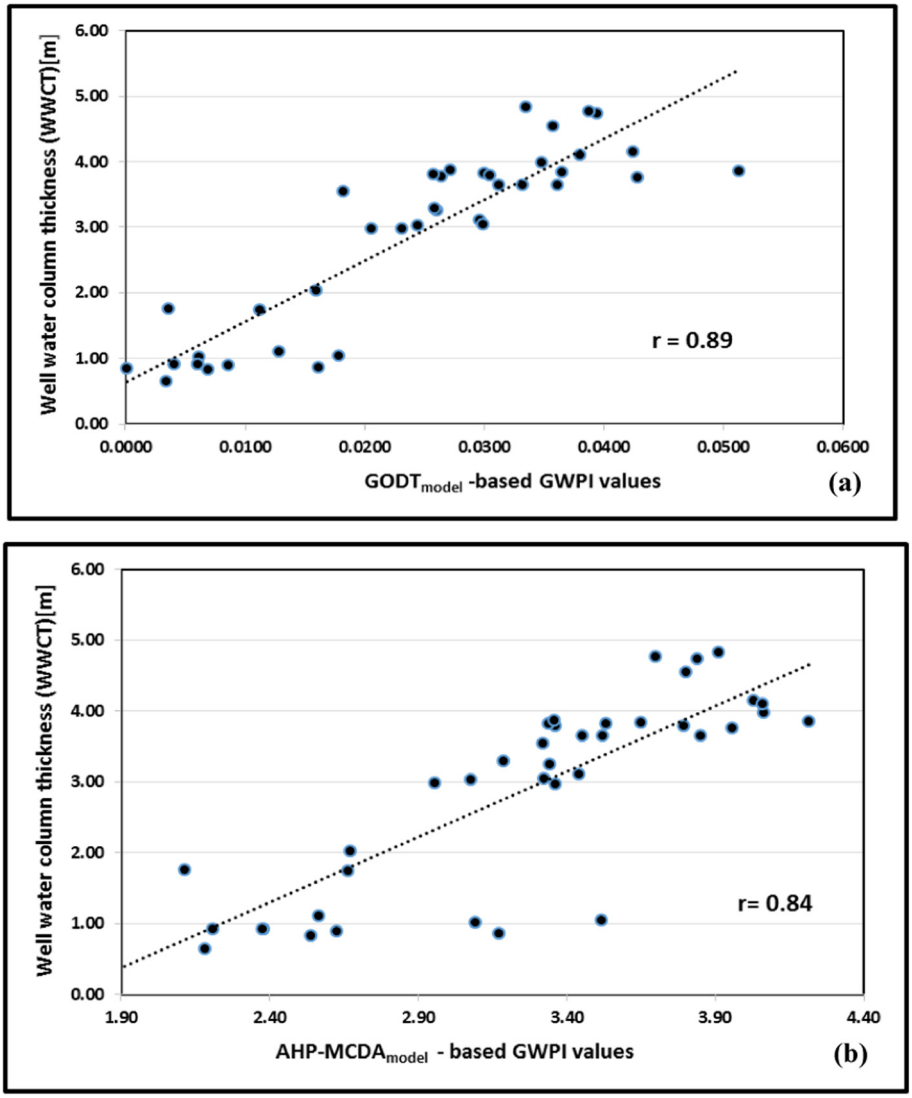

Fig. 8. (a) Plot between GODT-based GWPI values and Well water column thickness (m), (b) plot between AHP-MCDA-based GWPI values and Well water column thickness (m).

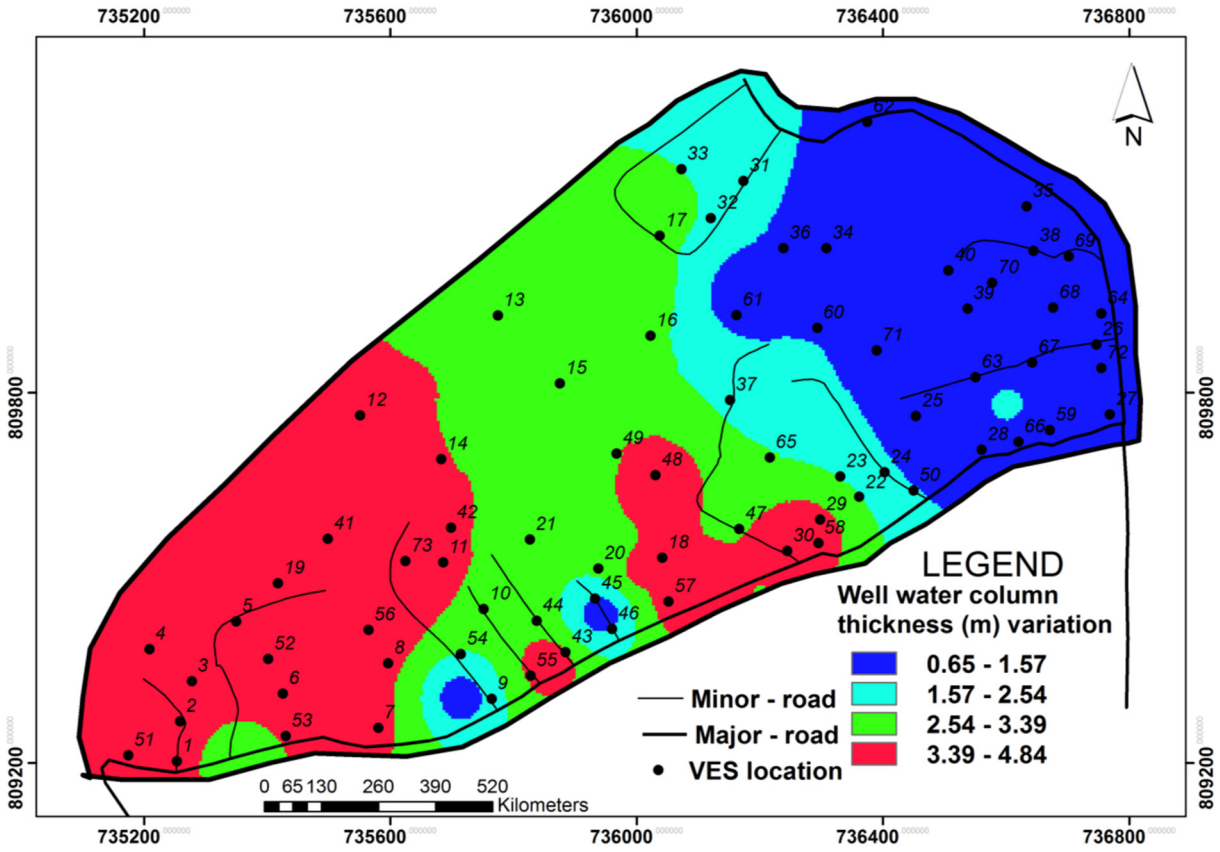

Fig. 9. Well water column thickness (WWCT) map of the study area.

based GWPI map, the area covered by the lows potential classes (L and LM) occupy 47% areas, meanwhile both M and H potential classes account for 29% and 24%, respectively.

4.4. Validation of the GPPI maps and the MCDA Models performance evaluation

The integral part of this study is to evaluate the reliability of a produced decision support system (DSS) tool for possible implementation in environmental decision making studies. As reported in the studies of Jha et al. (2010), Nampak et al. (2014), Mogaji and Lim (2017a), validation is the very apt scheme for establishing the reliability of any proposed DSS model in decision making process. Conventionally, the act of employing the step-drawdown test data and available yield data validation approaches would have been more appropriate for the produced GPPI maps validation, but the paucity of data is a constraint (Jha et al., 2010; Mogaji, 2016a,b). Therefore, a correlation technique approach as reported in the studies of Pradhan et al. (2013), Singh et al. (2014), Pearson (1900), Snedecor and Cochran (1980), that can allows scrutinizing the connection between two measurable and continuous variables is potentially explored. Likewise, the spatial attribute comparative scheme validation approach is also looked into in this study. In order to achieve this objective, the measured well data i.e. well water column thickness determined from the available hand dug wells in the investigated area as supported in the study of Akinlalu et al. (2017) were analyzed involving the correlating technique approach. For this approach, the GIS spatial analyst tool was used for extracting the spatial pixel values of the spatially modeled well water column thickness estimates against the corresponding estimated values of GODT-based GWPI at each VES locations in the area. The results obtained were used to developed correlations graph plots. Fig. 8a represent the plots of the 73 correlated data pairs between the well water column thickness estimates and the GODT-based GWPI estimates. According to the plots, the regression coefficient 'r' for the quantitative relationship between the GODT model-based GWPI values and well water column thickness values is 89% (Fig. 8a). Further, the spatial attribute comparative scheme (SACS) on the other hand is experimented following the similar approach documented in the studies of Manap et al. (2011), Mogaji et al. (2015a), Mogaji and Lim (2016). The SACS entails validating the groundwater conceptual model map produced (Fig. 6) through qualitative comparison of the predicted potential zones' attributes with the produced well water column thickness (WWCT) map (Fig. 9). Using the spatial attributes boundary classes of range 0.65–1.57, 1.57–2.54, 2.54–3.39 and 3.39–4.84 according to Fig. 9, the WWCT values observed at each located hand-dug well (See column 4 of Table 10) were calibrated and qualitatively compared with the spatial attribute of the predicted potential zones on the GPPI model map (Fig. 6). The results of this analysis gives the validation results presented in Table 10. According to Table 10, the prediction accuracy of the produced GODT model-based GPPI map was quantitatively evaluated to provide 72.5% prediction capability. Applying the aforementioned discussed validation approaches, the AHP-based GWPI produced GPPI map (Fig. 7) was also validated to give the regression coefficient 'r' of 84% (Fig. 8b) for the former approach and 65% for the latter approach. The resulting line of fit which show positive correlation between the GODT model-based GWPI values and AHP-MCDA-based GWPI values and well water column thickness values validated the performance evaluation of both proposed GODT model and the applied AHP-MCDA model.

Table 10
The spatial attribute comparative scheme qualitative result.

Well no	Observed coordinates		WWCT determined	Attributes comparison Remark	
	Long	Lat		GODT model-based GPPI map	AHP model-based GPPI map
1	735858.2	809357.8	3.83	Disagree	Agree
2	735557.3	809454.4	4.84	Agree	Agree
3	735381.2	809357.8	3.77	Agree	Agree
4	736664.6	809744	0.85	Agree	Agree
5	736605	809780.9	1.76	Disagree	Disagree
6	736485.7	809914.3	0.65	Agree	Agree
7	736042.8	810110.3	3.04	Agree	Agree
8	735188.01	809464.27	3.65	Disagree	Disagree
9	735943.98	809441.31	1.02	Agree	Disagree
10	735146.2	809420.6	3.79	Disagree	Disagree
11	736005.87	809510.83	3.55	Disagree	Disagree
12	735373.44	809634.23	4.75	Agree	Agree
13	735789.16	809824.25	2.99	Agree	Disagree
14	736270.81	809565.07	3.99	Agree	Agree
15	736037.54	809660.1	3.86	Agree	Agree
16	736182.05	809958.5	0.83	Agree	Disagree
17	736543.26	810143.21	0.92	Agree	Agree
18	735893.55	809697.54	3.26	Agree	Agree
19	735151.79	809322.28	3.82	Agree	Disagree
20	736403.7	810163.73	1.11	Disagree	Disagree
21	735447.32	809396.16	3.65	Disagree	Agree
22	736366.76	810048.8	0.89	Agree	Disagree
23	735714.12	809305.86	1.05	Agree	Disagree
24	735373.44	809634.23	3.12	Disagree	Disagree
25	736243.62	809823.05	1.75	Disagree	Agree
26	736654.09	809855.88	0.87	Agree	Disagree
27	736502.22	809745.06	0.92	Agree	Agree
28	735623.82	809896.93	3.05	Agree	Agree
29	735529.42	809334.59	3.8	Agree	Agree
30	735554.04	809260.71	3.65	Agree	Agree
31	736530.95	810135	0.92	Agree	Agree
32	736132.8	810200.67	2.03	Agree	Agree
33	735533.52	809531.62	4.15	Agree	Agree
34	735357.02	809211.45	2.98	Agree	Agree
35	736075.33	809470.05	4.1	Agree	Agree
36	735986.3	809983.13	3.3	Agree	Agree
37	735205.15	809277.13	3.88	Agree	Agree
38	735447.32	801396.16	4.77	Disagree	Agree
39	735586.8	809843.51	3.84	Agree	Agree
40	735151.79	809322.28	4.55	Disagree	Disagree

WWCT: Well water column thickness.

In addition, from the perspective of multi-faceted geology (Fig. 1c) correlation with the produced GPPI maps (Figs. 6 and 7), the predicted high and medium potential zones in these maps were observed underlain by the quarzitic rock type. The low potential zone on the other hand is found covering the charnokitic rock type area while low medium and small patches of low potential zones sheltered the granite rock type region. In accordance with Ojo et al. (2011), geologic features such as faults and shear zones are often associated with the quarzitic rocks region whose weathering products is sandy. The resulting sandy weathering product and those possible geologic features often enhanced secondary porosity creation and good aquifer material development which could have contributed to groundwater potentiality and occurrences of the predicted high and medium zones in the area. In a charnokitic rocky area, the soil weathering product is clayey material. According to Mogaji and Lim (2017a), clayey formation is impervious and its physical properties are low porosity and negligible permeability which make it a bad aquifer material that can only support low potential yield rating. With this geological correlated results, the MCDA model's produced GPPI maps are further validated. Sequel to the above validation results, the proposed GODT model's reliability for decision making process is further established including the prediction capability of the applied MCDA–AHP technique.

5. Conclusion

Water is one of the most precious natural resources needed for man's existence. Surface water being the most often available source of water is not always in the right place, at the right time and of the right quality. Hence, the need arises to consider groundwater as an alternative source of water resource supply. Groundwater potentiality zones mapping is an important measures in groundwater resources sustainable development. Several multi-criteria decision analysis (MCDA) approaches have been deployed by numerous researchers for effective analysis in this regard. To increase developing decision support model tool in the field of groundwater hydrology, a new MCDA-GODT modeling algorithm is proposed. The application of the GODT model is investigated for groundwater potentiality mapping in a typical crystalline multi-faceted geologic terrain, southwestern, Nigeria. The decision support model map produced with the applied GODT modeling method were compared with the applied results of the conventional AHP–MCDA modeling method to a real-world case study setting. The produced groundwater potentiality prediction index (GPPI) maps based on these MCDA approaches classified the area into four potential zones. To produce the GPPI maps, the first step was to derive four groundwater potential conditioning factors (GPCFs)-hydro-geologic parameters (Groundwater hydraulic con-

finement, Aquifer overlying strata, Depth to water table and Aquifer thickness for implementing the GODT modeling algorithm. These GPCFs were obtained from the interpreted 73 Schlumberger depth sounding data acquired in the study area. The derived GPCFs were converted to hydro-geologic theme parameters in GIS platform and used as input to GODT and AHP-MCDA modeling mechanisms. The GODT and AHP-MCDA modeling algorithms were applied to synthesize the GPCFs hydrologic themes and estimated both GODT model-based GWPI values and AHP-MCDA model-based GWPI values, respectively. The estimated GWPI values record were processed in GIS environment to produce GODT model-based GPPI map and AHP-MCDA model-based GPPI map for the study area. The reliability and precision of the produced GPPI maps for decision making were validated using both well data sets and surface geologic correlation approaches. The regression correlation coefficient results based on the well data analyzed approach established 89% and 84% for GODT model and AHP-MCDA model, respectively. Similarly, the validation approach based on the spatial attribute comparative scheme (SACS) also yielded 72.5% and 65% for these data mining models, respectively. The qualitative correlation results of the geologic rock units with the predicted potential zones also revealed good agreement for these DSS models. The produced groundwater potentiality prediction index (GPPI) maps can provide valuable information for hydrogeologist, planners, and decision makers to put suitable plans for sustainability development of groundwater resource in the study area. Finally, based on this study, it can be concluded that the proposed MCDA–GODT modeling algorithm method give more reliable results in groundwater potentiality assessment in a multifaceted geologic terrain. Hence, this method can be used routinely in groundwater exploration in favourable geological conditions.

References

Adeyemo, I.A., Mogaji, K.A., Olowolafe, T.S., Fola-Abe, A.O., 2015. Groundwater vulnerability modelling from geoelectrical derived parameters-case of GIS-based GODA model approach. Int. J. Petrol. Geosci. Eng. 03 (02), 69–80.

Adiat, K.A.N., Nawawi, M.N.M., Abdullah, K., 2012. Assessing the accuracy of GIS-based elementary multi criteria decision analysis as a spatial prediction tool – a case of predicting potential zones of sustainable groundwater resources. J. Hydrol. 440, 75–89. http://dx.doi.org/10.1016/j.jhydrol.2012.03.028.

Adiat, K.A.N., Nawawi, M.N.M., Abdullah, K., 2013. Application of multi-criteria decision analysis to geoelectric and geologic parameters for spatial prediction of groundwater resources potential and aquifer evaluation. Pure Appl. Geophys. 170, 453–471. http://dx.doi.org/10.1007/s00024-012-0501-9.

Akinlalu, A.A., Adegbuyiro, A., Adiat, K.A.N., Akeredolu, B.E., Lateef, W.Y., 2017. Application of multi-criteria decision analysis in prediction of groundwater resources potential: a case of Oke-Ana, Ilesa Area Southwestern, Nigeria. NRIAG J. Astron. Geophys.

Al-Saud, M., 2010. Mapping potential areas for groundwater storage in Wadi Aurnah Basin, western Arabian Peninsula, using remote sensing and geographic information system techniques. Hydrogeol. J. 18, 1481–1495.

Andreo, B., Viras, J.M., Perles, M.J., Carrasco, F., 2005. A comparative study of four schemes for groundwater vulnerability mapping in a diffuse flow carbonate aquifer under Mediterranean climatic conditions. Environ. Geol. 2005 (47), 586–595. http://dx.doi.org/10.1007/s00254-004-1185-y.

Anomohanran, O., Ofomola, M.O., Okocha, F.O., 2017. Investigation of groundwater in parts of Ndokwa District in Nigeria using geophysical logging and electrical resistivity methods: implications for groundwater exploration, m. J. Afr. Earth Sc. 129, 108–116.

Awawdeh, M., Obeidat, M., Al-Mohammad, M., Al-Qudah, K., Jaradat, R., 2014. Integrated GIS and remote sensing for mapping groundwater potentiality in the Tulul Al Ashaqif, Northeast Jordan. Arab. J. Geosci. 7 (6), 2377–2392.

Bala, A.N., Ike, E.C., 2001. The aquifer of the crystalline basement rocks in Gusau area, North-western *Nigeria*. J. Min. Geol. 37 (2), 177–184.

Banks, D., Karnachuk, O.V., Parnachev, V.P., Holden, W., Frengstad, B., 2002. Rural pit latrines as a source of groundwater contamination; examples from Siberia and Kosova. J. Chart. Inst. Water Environ. Manage. 2002 (16), 147–152.

Bates, B.C., Kundzewicz, Z.W., Wu, S., Palutikof, J., 2008. Climate change and water Technical paper of the Intergovernmental Panel on Climate Change. IPCC Secretariat, Geneva.

Carranza, E.J.M., Van Ruitenbeek, F.J.A., Hecker, C., Van Der Meijde, M., Van der Meer, F.D., 2008. Knowledge-guided data-driven evidential belief modeling of mineral prospectivity in Cabo de Gata, SE Spain. Int. J. Appl. Earth Obs. Geoinform. 10 (3), 374–387.

Cheng-Haw, L., Chih-Chao, H., Hsin-Fu, Y., Hung-I, L., Shing-Tsz, L., Kuo-Chin, H., 2013. Groundwater recharge and exploitative potential zone mapping using GIS and GOD techniques. Environ. Earth Sci. 2013 (68), 267–280. http://dx.doi.org/10.1007/s12665-012-1737-5.

Chowdhury, A., Jha, M.K., Chowdary, V.M., Mal, B.C., 2009. Integrated remote sensing and GIS-based approach for assessing groundwater. Int. J. Remote Sens. 30 (1), 231–250.

Corsini, A., Cervi, F., Ronchetti, F., 2009. Weight of evidence and artificial neural networks for potential groundwater mapping: an application to the Mt. Modino area (Northern Apennines, Italy). Geomorphology 111, 79–87. http://dx.doi.org/10.1016/j.geomorph.2008.03. 015.

Dan-Hassan, N.A., Olorunfemi, M.O., 1999. Hydro- geophysical investigation of a basement terrain in the north central part of Kaduna State Nigeria. J. Min. Geol. 35 (2), 189–206.

Dhar, A., Sahoo, S., Dey, S., Sahoo, M., 2014. Evaluation of recharge and groundwater dynamics of a shallow alluvial aquifer in central ganga basin, Kanpur (India). Nat. Resour. Res. 23, 409–422.

Elmahdy, S.I., Mohamed, M.M., 2014. Probabilistic frequency ratio model for groundwater potential mapping in Al Jaww plain, UAE. Arab. J. Geosci. http://dx.doi.org/10.1007/s12517-014-1327-9.

Faleye, E.T., Olorunfemi, M.O., 2015. Aquifer characterization and groundwater potential assessment of the sedimentary basin of Ondo state Ife. J. Sci. 17 (2), 2015.

Fitterman, D.V., Deszcz-Pan, M., Prinos, S.T., 2012. Helicopter electromagnetic survey of the Model Land Area, Southeastern Miami-Dade County, Florida. U.S. Geological Survey Open-File Report 2012 (1176), 77.

Fitts, C.R., 2002. Groundwater Science. Academic, San Diego.

Foster, S.S.D., 1987. Fundamental concept in aquifer vulnerability, pollution and protection strategy. In: Van Duijveribooden, W., Van Waegeningh, G.H. (Eds.), TNO Committee on Hydrological Research, the Hague, Proceedings and Information, vol. 38, pp. 69–86.

Gruba, W., Rieger, R., 2003. High resolution seismic reflection – constraints and pitfall in groundwater exploration. RMZ-Mater. Geoenviron. 50 (1), 133–136.

Gorai, A.K., Pathak, G., Iqua, J., 2014. Development of hierarchical fuzzy model for groundwater vulnerability to pollution. Arab. J. Geosci. http://dx.doi.org/10.1007/a12517-014-1417-8.

Hinnell, A.C., Ferre, T.P.A., Vrugt, J.A., Huisman, J.A., Moysey, S., Rings, J., Kowalsky, M.B., 2010. Improved extraction of hydrologic information from geophysical data through coupled hydrogeophysical inversion. Water Resour. Res. http://dx.doi.org/10.1029/2008WR007060.

Jayeoba, A., Oladunjoye, M.A., 2013. Hydro-geophysical evaluation of groundwater potential in hard rock terrain of southwestern Nigeria. RMZ – M&G 60, 271–285.

Jha, M.K., Chowdhury, A., Chowdary, V.M., Peiffer, S., 2007. Groundwater management and development by integrated remote sensing and geographic information systems: prospects and constraints. Water Resour. Manag. 21 (2), 427–467.

Jha, M., Chowdary, V., Chowdhury, A., 2010. Groundwater assessment in Salboni Block, West Bengal (India) using remote sensing, geographical information system and multi-criteria decision analysis techniques. Hydrogeol. J. 18, 1713–1728. http://dx.doi.org/10.1007/s10040-010-0631-z.

Jupp, D.L.B., Vozoff, K., 1975. Joint inversion of geophysical data. Geophys. J. Roy. Astron. Soc. 1975 (42), 977–991.

Kayode, J.S., Adelusi, A.O., Nawawi, M.N.M., Bawallah, M., Olowolafe, T.S., 2016. Geo-electrical investigation of near surface conductive structures suitable for groundwater accumulation in a resistive crystalline basement environment: a case study of Isuada, southwestern Nigeria. J. Afr. Earth Sci. 119, 289–302.

Khemiri, S., Khnissi, A., Alaya, M.B., Saidi, S., Zargouni, F., 2013. Using GIS for the comparison of intrinsic parametric methods assessment of groundwater vulnerability to Pollution in Scenarios of Semi-Arid Climate. Case Foussana Groundwater Cent. Tunisia J. Water Resour. Prot. 5, 835–845.

MachiwaL, D., Jha, M.K., 2014. Characterizing rainfall-groundwater dynamics in a hard-rock aquifer system using time series, geographic information system and geostatistical modelling. Hydrol. Process. 28, 2824–2843.

Machiwal, D., Singh, P.K., 2015. Comparing GIS-based multi-criteria decision-making and Boolean logic modelling approaches for delineating groundwater recharge zones. Arab. J. Geosci. 2015 (8), 10675–10691. http://dx.doi.org/10.1007/s12517-015-2002-5.

Machiwal, D., Madan, K.J., Bimal, C.M., 2010. Assessment of groundwater potential in a semi-arid region of India using remote sensing, GIS and MCDM techniques. Water Resour. Manage. 25, 1359–1386.

Manap, M.A., Sulaiman, W.N.A., Ramli, M.F., Pradhan, B., Surip, N., 2011. A knowledge-driven GIS modelling technique for groundwater potential mapping at the Upper Langat Basin, Malaysia. Arab. J. Geosci. 6 (5), 1621–1637. http://dx.doi.org/10.1007/s12517-011- 0469-2.

McKay, G., Harris, J.R., 2015. Comparison of the data-driven random forests model and a knowledge-driven method for mineral prospectively mapping: a case study for gold deposits around the Huritz Group and Nueltin Suite, Nunavut, Canada. Nat. Resour. Res. http://dx.doi.org/10.1007/s11053-015-9274-z.

Meijerink, A.M.J., 2007. Remote sensing applications to groundwater IHP-VI. Series on Groundwater No. 16. UNESCO, Paris.

Mogaji, K.A., Olayanju, G.M., Oladapo, M.I., 2011. Geophysical evaluation of rock types impact on aquifer characterisation in the basement complex areas of

Ondo state, Southwestern, Nigeria: geo-electric assessment and geographic information approach. Int. J. Water Resour. Environ. Eng. 3 (4), 77–86.
Mogaji, K.A., Lim, H.S., Abdullah, K., 2013. Regional modeling of climate change impacts on groundwater resources sustainability in Peninsular Malaysia. Mod. Appl. Sci. 7 (5). ISSN 1913–1844 E-ISSN 1913–1852Published by Canadian Center of Science and Education.
Mogaji, K.A., Lim, H.S., Abdullah, K., 2015a. Regional prediction of groundwater potential mapping in a multifaceted geology terrain using GIS-based Dempster-Shafer model. Arab. J. Geosci. 8, 3235–3258. http://dx.doi.org/10.1007/s12517014-1391-1.
Mogaji, K.A., Lim, H.S., Abdullah, K., 2015b. Modeling of groundwater recharge using a multiple linear regression (MLR) recharge model developed from geophysical parameters: a case of groundwater resources management. Environ. Earth Sci. http://dx.doi.org/10.1007/s12665-014-3476-.
Mogaji, K.A., 2016a. Geoelectrical parameter-based multivariate regression borehole yield model for predicting aquifer yield in managing ground water resource sustainability. J. Taibah Univ. Sci. 10 (2016), 584–600.
Mogaji, K.A., 2016b. Combining geophysical techniques and multi-criteria GIS-based application modeling approach for groundwater potential assessment in southwestern Nigeria. Environ. Earth Sci. 75, 1181. http://dx.doi.org/10.1007/s12665-016-5897-6.
Mogaji, K.A., Lim, H.S., 2016. Groundwater potentiality mapping using geoelectrical-based aquifer hydraulic parameters: a GIS-based multi-criteria decision analysis modeling approach. Terr. Atmos. Ocean Sci. http://dx.doi.org/10.3319/TAO.2016.11.01.02.
Mogaji, K.A., 2017. Development of AHPDST vulnerability indexing model for groundwater vulnerability assessment using hydrogeophysical derived parameters and GIS application. Pure Appl. Geophys. 2017 (174), 1787–1813. http://dx.doi.org/10.1007/s00024-017-1499-9.
Mogaji, K.A., Lim, H.S., 2017a. Development of groundwater favourability map using GIS-based driven data mining models: an approach for effective groundwater resource management. Geocarto Int. http://dx.doi.org/10.1080/10106049.2016.1273400.
Mogaji, K.A., Lim, H.S., 2017b. Application of a GIS-/remote sensing-based approach for predicting groundwater potential zones using a multi-criteria data mining methodology. Environ. Monit. Assess 189, 321. http://dx.doi.org/10.1007/s10661-017-5990-7.
Mohamed, S.E.J., Shaharin, I., Wan, N.A.S., Puziah, A.L., 2012. Groundwater resources assessment using integrated geophysical techniques in the southwestern region of Peninsular Malaysia. Arab. J. Geosci. 6 (11), 4129–4144.
Murthy, K.S.R., 2000. Groundwater potential in a semi-arid region of Andhra Pradesh: a GIS approach. Int. J. Remote Sens. 21 (9), 1867–1884.
Naghibi, S.A., Pourghasemi, H.R., Pourtaghi, Z.S., Rezaei, A., 2015. Groundwater qanat potential mapping using frequency ratio and Shannon's entropy models in the Moghan watershed. Iran Earth Sci. Inform. 8, 171–186.
Nampak, H., Pradhan, B., Manap, M.A., 2014. Application of GIS based data driven evidential belief function model to predict groundwater potential zonation. J. Hydrol. 513, 283–300.
Ndatuwong, L.G., Yadav, G.S., 2014. Application of geo-electrical data to evaluate groundwater potential zone and assessment of overburden protective capacity in part of Sonebhadra district, Uttar Pradesh. Environ. Earth Sci. http://dx.doi.org/10.1007/s12665-014-3649-z.
Oborie, E., Udom, G.J., 2014. Determination of aquifer transmissivity using geoelectrical sounding and pumping test in pats of Bayelsa State, Nigeria. J. Phys. Environ. Sci. Res. 2 (2), 32–40.
Ojo, J.S., Olorunfemi, M.O., Falebita, D.E., 2011. An appraisal of the geologic structure beneath the Ikogosi warm spring in south-western Nigeria using integrated surface geophysical methods. Earth Sci. Res. SJ 15 (1), 27–34. July 2011Resea.
Oh, H.J., Kim, Y.S., Choi, J.K., Park, E., Lee, S., 2011. GIS mapping of regional probabilistic groundwater potential in the area of Pohang City, Korea. J. Hydrol. 399, 158–172.
Oladapo-Adeoye, O.O., Mogaji, K.A., Oladapo, M.I., 2015. Multi-array hydro-geoelectric characterization of a crystalline basement complex environment. Phys. Sci. Int. J. 8 (2), 1–18. Article no.PSIJ.17444ISSN: 2348–0130.
Olayanju, G.O., Mogaji, K.A., Lim, H.S., Ojo, T.S., 2017. Foundation integrity assessment using integrated geophysical and geotechnical techniques: case study in crystalline basement complex, southwestern Nigeria. J. Geophys. Eng. 14 (2017), 675–690.
Olorunfemi, M.O., Fasuyi, S.A., 1993. Aquifer types and the geoelectric/hydrogeologic characteristics of part of central basement terrain of Nigeria (Niger State). J. Afr. Earth Sci. 16 (3), 309–317.
Orellana, E., Mooney, H.M., 1966. Master Tables and Curves for Vertical Electrical Sounding Over Layered Structures. Interciencia, Madrid, Spain.
Oseji, J., Ofomola, M., 2010. Determination of groundwater flow direction in Utagba Ogbe Kingdom, Udukwa Land Area of Delta State, Nigeria. J. Earth Sci. 4 (1), 32–34.
Park, I., Yongsung, K., Saro, L., 2014. Groundwater productivity potential mapping using evidential belief function. Groundwater 52, 201–207. Focus Issue.
Pathak, G., Iqba, J., Gorai, A.K., Katpata, Y.B., 2015. Development of GIS-based fuzzy pattern recognition model (modified DRASTIC model) for groundwater vulnerability to pollution assessment. Int. J. Environ. Sci. Technol. http://dx.doi.org/10.1007/s13762-014-0693-x.
Pearson, K., 1900. On the criterion that a given system of deviations from the probable in the case of a correlated system of variables is such that it can be reasonably supposed to have arisen from random sampling. Philos. Mag. 5 (50), 157–175. reprinted in K. Pearson (1956), pp 339–357.
Pradhan, B., Neshat, A., Pirasteh, S., Shafri, H.Z.M., 2013. Estimating groundwater vulnerability to pollution using a modified DRASTIC model in the Kerman agricultural area, Iran. Environ. Earth Sci. http://dx.doi.org/10.1007/s12665-013-2690-7.
Rahmati, O., Pourghasemi, H.R., Melesse, A.M., 2016. Application of GIS-based data driven random forest and maximum entropy models for groundwater potential mapping: a case study at Mehran Region, Iran. Catena 137, 360–372.
Rijkswatersta, A.T., 1969. Standard Graphs for Resistivity Prospecting; European Association of Exploration Geophysicists. Hague, The Netherlands.
Saaty, T.L., Vargas, G.L., 1991a. Prediction, Projection and Forecasting. Kluwer, Dordrecht.
Saraf, A.K., Choudhury, P.R., 1998. Integrated remote sensing and GIS for groundwater exploration and identification of artificial recharge sites. Int. J. Remote Sens. 19 (10), 1825–1841.
Saaty, T.L., Vargas, G.L., 1991b. Prediction, Projection and Forecasting. Kluwer Academic Publishers, Dordrecht.
Sahoo, M., Sahoo, S., Dhar, A., Pradhan, B., 2016. Effectiveness evaluation of objective and subjective weighting methods for aquifer vulnerability assessment in urban context. J. Hydrol. 541 (2016), 1303–1315.
Satpathy, B.N., Kanungo, B.N., 1976. Groundwater exploration in Hard rock terrain – a case study. Geophys. Prospect. 24 (4), 725–763.
Sharma, S.P., Barawal, V.C., 2005. Delineation of groundwater – bearing fractures zone in hardrock area integrating very low frequency electromagnetic and resistivity data. J. Appl. Geophys. 2005 (57), 155–166.
Singh, A., Srivastav S.K., Kumar, S., Chakrapani, G.J., 2014. A modified-DRASTIC model (DRASTICA) for assessment of groundwater vulnerability to pollution in an urbanized environment in Lucknow, India. Environ. Earth Sci. http://dx.doi.org/10.1007/s12665-015-4558-5.
Snedecor, G.W., Cochran, W.C., 1980. Correlation. Statistical Methods. The Iowa State University Press, Ames, Iowa, USA, pp. 171–198.
Srivastava, P.K., Gupta, M., Mukherjee, S., 2012. Mapping spatial distribution of pollutants in groundwater of a tropical area of India using remote sensing and GIS. Appl. Geomatics 4 (1), 21–32.
Sultan, S.A., Santos, F.M., 2009. Combining TEM/resistivity joint inversion and magnetic data for groundwater exploration: application to the northern part of Greater Cairo, Egypt. Environ. Geol. 2009 (58), 521–529.
Todd, D.K., 2004. Ground Water Hydrology. John Wiley & Sons, New York.
Vander-Velper, B.P.A., 2004. WinRESIST Version 1.0 Resistivity Depth SoundingInterpretation Software M. Sc Research Project. ITC, Delft Netherland.
Vladimir, F., Itay, S., Michael, F., Arie, A., 2017. Leachate detection via statistical analysis of electrical resistivity and induced polarization data at a waste disposal site (Northern Israel). Environ. Earth Sci. 76, 233. http://dx.doi.org/10.1007/s12665-017-6554-4.
Zhou, l., Chen, Y., 2014. Exploring the potential of community-based grassland management in Yanchi County of Ningxia Hui Autonomous Region, China: an application of the SWOT-AHP method. Environ. Earth Sci. 2014 (72), 1811–1820. http://dx.doi.org/10.1007/s12665-014-3090-3.